The Plant Cell, Vol. 29: 526–542, March 2017, www.plantcell.org

Regulation of Stomatal Immunity by Interdependent Functions of a Pathogen-Responsive MPK3/MPK6 Cascade and Abscisic Acid

Jianbin Su,[a,b] Mengmeng Zhang,[a] Lawrence Zhang,[c,1] Tiefeng Sun,[a] Yidong Liu,[b] Wolfgang Lukowitz,[d] Juan Xu,[a,2] and Shuqun Zhang[a,b,2]

[a] Key Laboratory of Plant Physiology and Biochemistry, College of Life Sciences, Zhejiang University, Hangzhou, Zhejiang 310058, China

[b] Division of Biochemistry, Interdisciplinary Plant Group, Bond Life Sciences Center, University of Missouri, Columbia, Missouri 65211

[c] David H. Hickman High School, Columbia, Missouri 65203

[d] Department of Plant Biology, University of Georgia, Athens, Georgia 30602

ORCID IDs: 0000-0002-1201-0076 (J.S.); 0000-0003-3207-498X (M.Z.); 0000-0002-3401-7893 (Y.L.); 0000-0002-5864-7240 (W.L.); 0000-0001-6683-6415 (J.X.); 0000-0003-2959-6461 (S.Z.)

Activation of mitogen-activated protein kinases (MAPKs) is one of the earliest responses after plants sense an invading pathogen. Here, we show that MPK3 and MPK6, two *Arabidopsis thaliana* pathogen-responsive MAPKs, and their upstream MAPK kinases, MKK4 and MKK5, are essential to both stomatal and apoplastic immunity. Loss of function of *MPK3* and *MPK6*, or their upstream *MKK4* and *MKK5*, abolishes pathogen/microbe-associated molecular pattern- and pathogen-induced stomatal closure. Gain-of-function activation of MPK3/MPK6 induces stomatal closure independently of abscisic acid (ABA) biosynthesis and signaling. In contrast, exogenously applied organic acids such as malate or citrate are able to reverse the stomatal closure induced by MPK3/MPK6 activation. Gene expression analysis and in situ enzyme activity staining revealed that malate metabolism increases in guard cells after activation of MPK3/MPK6 or inoculation of pathogen. In addition, pathogen-induced malate metabolism requires functional MKK4/MKK5 and MPK3/MPK6. We propose that the pathogen-responsive MPK3/MPK6 cascade and ABA are two essential signaling pathways that control, respectively, the organic acid metabolism and ion channels, two main branches of osmotic regulation in guard cells that function interdependently to control stomatal opening/closure.

INTRODUCTION

For successful pathogenesis, the pathogen must gain entry into the interior of the plant to acquire nutrients. Some pathogenic fungi secrete digestive enzymes or use mechanical force to overcome the impermeable cuticle layer that covers most parts of the plants, yet most other pathogens can only gain entry through wounds or natural openings such as hydathodes or stomatal pores (Grimmer et al., 2012). As a countermeasure, plants can rapidly close their stomata upon perception of pathogens to restrict pathogen entry, a response known as stomatal immunity (Melotto et al., 2006). Once pathogens overcome the surface barrier and enter the interior space of leaves, the perception of pathogen invasion by host cells induces rapid strengthening of their cell walls and secretion of a set of antimicrobial molecules and/or compounds to the apoplastic region to suppress pathogen growth, a process known as apoplastic immunity (Monaghan and Zipfel, 2012; Doehlemann and Hemetsberger, 2013). Plants have surface pattern recognition receptors to perceive pathogen/microbe-associated molecular patterns (PAMPs), which initiates an array of defense signaling events including activation of mitogen-activated protein kinases (MAPKs), Ca^{2+} influx, reactive oxygen species (ROS) burst, NO production, and activation/inhibition of ion channels (Ausubel, 2005; Chisholm et al., 2006; Jones and Dangl, 2006; Boller and Felix, 2009; Böhm et al., 2014). These signaling events function independently or interdependently to form an intricate signaling network to ensure robust stomatal and apoplastic immunity (Melotto et al., 2008; McLachlan et al., 2014; Arnaud and Hwang, 2015).

Abscisic acid (ABA) plays an important role in controlling plant water balance by regulating stomatal opening and closure (Hetherington and Woodward, 2003; Kim et al., 2010; Ruszala et al., 2011; Chater et al., 2014). It is also essential to stomatal defense during plant immunity (Melotto et al., 2006; Zeng and He, 2010; Du et al., 2014; Lim et al., 2014). A recent study concluded that ABA and PAMP (flg22) signals converged at slow anion channel-associated 1 (SLAC1) and ABA signaling plays only a minor role in stomatal defense (Montillet et al., 2013). By using a noninvasive nanoinfusion technique, another study demonstrated that ABA- and flg22-induced stomatal closure converge at the level of OST1 and then activate downstream SLAC1 and SLAH3 ion channels (Guzel Deger et al., 2015). ROS bursts play important roles in ABA- and PAMP-induced stomatal closure.

[1] Current address: School of Medicine, University of Missouri, Kansas City, MO 64108.

[2] Address correspondence to xujuan@zju.edu.cn or zhangsh@missouri.edu.

The author responsible for distribution of materials integral to the findings presented in this article in accordance with the policy described in the Instructions for Authors (www.plantcell.org) is: Juan Xu (xujuan@zju.edu.cn).

www.plantcell.org/cgi/doi/10.1105/tpc.16.00577

However, the mechanism of the PAMP-induced ROS burst is distinct from the ABA-induced ROS burst. Upon perception of PAMPs, the plasma-associated kinase BIK1 directly phosphorylates and activates the NADPH oxidase RbohD to induce ROS production (Kadota et al., 2014; Li et al., 2014). In contrast, ABA-induced ROS production is dependent on the kinase OST1 (Mustilli et al., 2002), which physically interacts with and phosphorylates RbohD/RbohF (Sirichandra et al., 2009; Acharya et al., 2013). MPK9 and MPK12, two guard cell-specific MAPKs that function downstream of ROS in ABA-mediated stomatal movement (Jammes et al., 2009), were also essential to plant resistance against spray-inoculated *Pseudomonas syringae* pv *tomato DC3000* (*Pst*) (Jammes et al., 2011). Interestingly, activation of EDS1/PAD4-dependent plant immune responses inhibits ABA-induced stomatal closure at the level of Ca^{2+} signaling (Kim et al., 2011), suggesting an intricate crosstalk between ABA signaling and plant immune networks. Besides ABA, salicylic acid (SA) biosynthesis and signaling are also required for pathogen/PAMP-induced stomatal closure (Melotto et al., 2006; Zeng and He, 2010; Zheng et al., 2012, 2015).

Plant pathogens also have several sophisticated strategies to interfere with plant stomatal immunity. Coronatine (COR), a phytotoxin produced by some strains of *P. syringae* (Cuppels and Ainsworth, 1995; Brooks et al., 2004), promotes stomatal reopening and inhibits ABA-induced stomatal closure (Melotto et al., 2006). COR hijacks the plant jasmonic acid receptor COI1 to activate several closely related NAC transcription factors, which subsequently prevents the accumulation of SA by inhibiting SA biosynthesis and promoting SA metabolism (Zheng et al., 2012; Du et al., 2014). In addition to COR, pathogen-secreted cytokinin (e.g., kinetin), fusicoccin, type III effectors, and oxalate also function differentially in counteracting plant stomatal immunity (Grimmer et al., 2012). Cytokinin exerts its inhibitory effect on ABA-induced stomatal closure through enhancing ethylene production (Tanaka et al., 2006), while fusicoccin directly stimulates plasma membrane-localized H^+-ATPases (Johansson et al., 1993). HopF2 and HopM1, two type III effectors secreted by *Pst*, were shown to inhibit stomatal immunity through inhibiting the PAMP-induced ROS burst (Hurley et al., 2014; Lozano-Durán et al., 2014).

Most interestingly, oxalate, an intermediate of the tricarboxylic acid (TCA) cycle, was shown to function as a virulence factor to counteract stomatal immunity by promoting accumulation of osmotically active molecules and inhibiting ABA-induced stomatal closure (Guimarães and Stotz, 2004). The finding of oxalate as a virulence factor indicates plant pathogens may counteract stomatal immunity by targeting guard cell organic acid metabolism to enhance pathogenicity. Malate, together with Cl^- and NO_3^-, are the major anions to balance the positively charged K^+ during stomatal opening (Kim et al., 2010; Araújo et al., 2011a). As a result, coordinated downregulation of guard cell organic and inorganic anions through metabolic conversion and transporter-mediated efflux could be an effective strategy to close stomata in response to various stimuli.

For a long time, the role of organic solutes was considered to be secondary in both stomatal closure and opening (Blatt, 2016). However, this viewpoint was challenged by three recent reports. One study found that guard cell triacylglycerol breakdown was essential to light-induced stomatal opening (McLachlan et al., 2016). It was proposed that triacylglycerol breakdown provided energy for plasma membrane localized H^+-ATPase. By using quantitative analysis of starch turnover and molecular genetic analyses, rapid starch degradation in guard cells was shown to play an important role in stomatal opening and plant fitness (Horrer et al., 2016). At the same time, the role of guard cell starch biosynthesis in stomatal closure was also reported (Azoulay-Shemer et al., 2016). Collectively, these recent studies highlight the essential role of metabolism in stomatal movement. These new findings also raise the question of how these metabolic processes are regulated during stomatal movement in response to various stimuli.

Arabidopsis thaliana MPK3, MPK4, and MPK6 are rapidly activated upon plant perception of PAMPs. They play critical roles in multiple plant defense responses (Meng and Zhang, 2013). It was shown that elevated MPK4 activity compromises Arabidopsis resistance to spray-inoculated *Pst*, but not *Pst*- or flg22-induced stomatal closure (Berriri et al., 2012). The role of MPK3 and MPK6 in regulating defense-related secondary metabolite biosynthesis has been intensively studied (Ren et al., 2008; Mao et al., 2011; Xu et al., 2016). Here, we show that MPK3 and MPK6, as well as their upstream kinases, MKK4 and MKK5, are essential to Arabidopsis immunity. They are involved in stomatal immunity by regulating guard cell primary organic acid metabolism. Loss of function of both *MPK3* and *MPK6* resulted in compromised stomatal immunity and high susceptibility phenotype of the double mutant. In contrast, *Pst*- and flg22-induced stomatal closure was not affected in *mpk3* or *mpk6* single mutant, which is consistent with their normal resistance against *Pst*. MPK3/MPK6 activation-induced stomatal closure is independent of ABA biosynthesis and signaling. It is also insensitive to COR, a phytotoxin capable of inhibiting ABA-induced stomatal closure. Our data suggest that MPK3 and MPK6 regulate stomatal immunity by controlling the metabolism of organic acids such as malate and citrate, well-known osmolytes in stomatal opening and closure. On the basis of these findings, we propose an interdependent model for MAPK and ABA signaling pathways in stomatal immunity.

RESULTS

Arabidopsis *MPK3* and *MPK6* Have Redundant Functions in Plant Immunity

MPK3 and MPK6, as well as their orthologs in other plant species, were believed to play positive roles in plant immunity based on their rapid activation by PAMPs and pathogen inoculation (Zhang and Klessig, 2001). They positively regulate various defense responses, including phytoalexin induction and defense gene activation (Ren et al., 2008; Mao et al., 2011; Meng and Zhang, 2013; Xu et al., 2016). However, clear genetic evidence to demonstrate a positive role of MPK3 and MPK6 in disease resistance is still lacking. Plants with *MPK6*, but not *MPK3*, suppressed by RNAi were reported to be more susceptible to *Pst*, with about a 1-log increase in pathogen growth (Menke et al., 2004). Pathogen resistance assays using *mpk3* or *mpk6* single mutants revealed that *mpk3*, but not *mpk6*, plants were more susceptible, with less than 1-log increase in *Pst* proliferation (Beckers et al., 2009). Our

repeated trials revealed no clear susceptible phenotype in *mpk3* single mutants and only a slightly higher bacterial growth in two independent *mpk6* mutant alleles ($0.01 < P < 0.05$) when spray- or infiltration-inoculated with *Pst* (Supplemental Figures 1A and 1C). Also, flg22-induced stomatal closure was normal in *mpk3* or two independent *mpk6* alleles (Supplemental Figure 1B). These contradictory results are likely a result of functional redundancy between MPK3 and MPK6, and the disease resistance phenotype of the *mpk3* or *mpk6* single mutant/RNAi line is subtle and subject to influence of experimental conditions.

MPK3 and MPK6 play redundant function in many developmental processes (Meng and Zhang, 2013; Xu and Zhang, 2015), including their essential function in embryogenesis. Previously, we generated a partially rescued *mpk3 mpk6* double mutant using a steroid-inducible promoter-driven *MPK6* (Wang et al., 2007). However, the rescued *mpk3 mpk6* double mutant seedlings lack normal pavement cells and cannot survive in soil; as a result, we could not examine the stomatal behavior and pathogen resistance of such mutant. Recently, using a chemical genetic approach, we generated another conditional *mpk3 mpk6* double mutant, named *MPK6SR* (genotype: *mpk3 mpk6* P_{MPK6}:*MPK6*^{YG}), in which *mpk3 mpk6* double mutant was rescued with MPK6^{YG}, a NA-PP1-sensitized version of MPK6. Replacement of Tyr-144 with Gly enlarges the ATP binding pockets of MPK6 and makes MPK6^{YG} sensitive to NA-PP1, a PP1 analog with a bulkier side chain (Xu et al., 2014). We also generated a similar system using a modified MPK3, MPK3^{TG}, and the rescued plants were named *MPK3SR* (genotype: *mpk3 mpk6* P_{MPK3}:*MPK3*^{TG}). NA-PP1-treated *MPK3SR* (line #64) and *MPK6SR* (line #58) plants were more susceptible to spray-inoculated *Pst* (Figures 1A and 1B), with close to 3-log increase in pathogen growth. In the absence of NA-PP1 inhibitor, both *MPK3SR* and *MPK6SR* plants behaved like wild-type (Col-0) control. In addition, Col-0 plants treated with NA-PP1 did not show increased susceptibility to *Pst*, demonstrating the specificity of NA-PP1 inhibitor to the chemical-sensitized MPK3 and MPK6. Similar results were observed in independent *MPK3SR* and *MPK6SR* lines (Supplemental Figure 2A).

We also tested *Pst* inoculation by syringe infiltration. As shown in Figures 1C and 1D, NA-PP1-treated *MPK3SR* (line #64) and *MPK6SR* (line #58) plants were more susceptible. Independent *MPK3SR* and *MPK6SR* lines also exhibited enhanced susceptibility (Supplemental Figure 3). In comparison to ~3 logs of more pathogen growth when *Pst* was spray-inoculated, infiltration inoculation only resulted in ~1 log of more *Pst* growth. This result suggests that MPK3 and MPK6 are involved in both stomatal and apoplastic immunity.

Arabidopsis *MPK3* and *MPK6* Play a Major Role in Stomatal Immunity

Consistent with our speculation based on two different pathogen inoculation methods, we observed that the clustered stomata are always wide open in the rescued *mpk3 mpk6* double mutants (Wang et al., 2007; Xu et al., 2014). These observations prompted us to examine the stomatal behavior in *MPK3SR* and *MPK6SR* plants after NA-PP1 treatment. The beauty of the chemical genetically rescued *MPK3SR* and *MPK6SR* plants is that we can allow the plants to grow and develop normally in the absence of inhibitor and then treat the plants with NA-PP1 to specifically block the kinase activity of the modified MPK3 or MPK6, which gives us activity null mutant of MPK3 and MPK6 for functional analyses. We found that stomatal closure in response to flg22 and *Pst* was impaired in both epidermal peels and intact leaves of *MPK3SR* and *MPK6SR* plants treated with NA-PP1 (Figures 1E and 1F; Supplemental Figure 4), indicating that reduced stomatal immunity contributes to the enhanced susceptibility of NA-PP1-treated *MPK3SR* and *MPK6SR* plants, i.e., *MPK3* and *MPK6* play essential function in plant stomatal immunity.

The best way to assess the levels of stomatal immunity is to quantify the number of pathogens that enter into the apoplastic spaces of leaves per stomata in a specific period of time. To achieve this, we developed a pathogen entry assay by utilizing the *luxCDABE*-tagged *Pst* strain (*Pst-lux*) (Fan et al., 2008) together with Photek photon-counting camera system, which can distinguish more than two orders of magnitude of *Pst-lux* bacteria (Supplemental Figure 5A). To remove the surface-attached *Pst-lux* cells, we washed the leaves in 0.02% Silwet L-77 with agitation. To assess the effectiveness, we pressed the washed leaves against *P. syringae* agar plates (Difco) and then cultured the plates for 24 h to generate "leaf prints." As shown in Supplemental Figure 5B, no *Pst-lux* was detected after 0.02% Silwet L-77 wash, indicating that the surface *Pst-lux* cells were removed efficiently, and the *Pst-lux* we detected in our pathogen entry assay resided inside leaves. We observed that more than 10-fold more *Pst-lux* bacteria entered into leaf interior of NA-PP1-treated *MPK3SR* and *MPK6SR* plants (Figures 2A and 2B). After being normalized to stomatal density (Figure 2C), the number of *Pst-lux* entered into the leaves of NA-PP1-treated *MPK3SR* and *MPK6SR* plants was >10 times more than those of the control plants (Figure 2D). Compromised stomatal immunity was also observed in independent *MPK6SR* and *MPK3SR* lines (Supplemental Figures 2B to 2E). Based on these data, we conclude that *MPK3* and *MPK6* have redundant functions in Arabidopsis stomatal immunity.

MKK4 and *MKK5* Play Redundant Roles in Both Stomatal and Apoplastic Immunity

Our previous study demonstrated that MKK4 and MKK5 are the MAPKKs upstream of MPK3/MPK6 in regulating stomatal development and patterning (Wang et al., 2007). To determine whether these two MAPKKs are also required for stomatal immunity, we generated *mkk4 mkk5* double mutants using the recently reported *mkk4* and *mkk5* single TILLING mutants (Zhao et al., 2014) after the *er-105* mutant allele was crossed away. Similar to the NA-PP1-treated *MPK3SR* and *MPK6SR* plants, the *mkk4 mkk5* double mutant plants were also highly susceptible to spray-inoculated *Pst* (Figures 3A and 3B). The *mkk4 mkk5* double mutant also exhibited impaired stomatal closure in response to flg22 and *Pst* (Figures 3C and 3D) and a higher level of *Pst-lux* entry (Figures 3E and 3F). We observed that the stomatal density of *mkk4 mkk5* double mutant was ~2.5 times higher than that of the wild type (Figure 3G) as a result of clustered stomata (Supplemental Figures 6A and 6B), which is consistent with our previous report (Wang et al., 2007). However, the clustered stomatal phenotype of this *mkk4 mkk5* double mutant is not as severe as the double

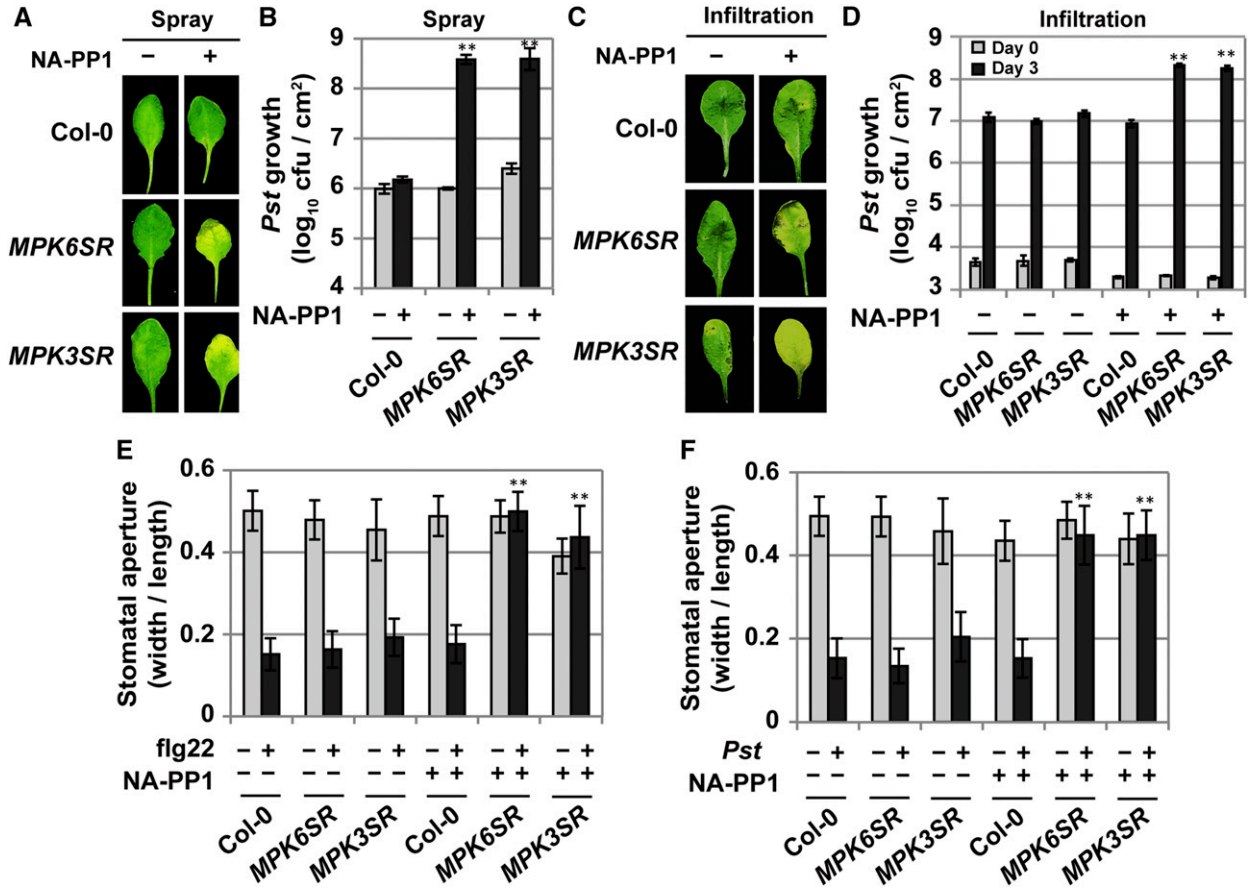

Figure 1. Arabidopsis *MPK3* and *MPK6* Play an Essential Role in Stomatal Immunity.

(A) and **(B)** Loss of function of *MPK3* and *MPK6* compromises plant resistance against *Pst*. Col-0, *MPK6SR* (line #58), and *MPK3SR* (line #64) plants were pretreated with DMSO (solvent control) or NA-PP1 (10 μM) for 3 h and then spray-inoculated with *Pst* (OD_{600} = 0.5). A second spray treatment of DMSO or NA-PP1 was performed 1.5 d post inoculation (dpi). Photos were taken at 3 dpi **(A)**, and bacterial growth was measured at 2.5 dpi **(B)**. Values are means ± SD, $^{**}P \leq 0.01$, $n = 3$. cfu, colony-forming units.

(C) and **(D)** Loss of function of *MPK3* and *MPK6* compromises apoplastic immunity. Col-0, *MPK3SR*, and *MPK6SR* plants were first spray with 10 μM NA-PP1 and then infiltration-inoculated with *Pst* (OD_{600} = 0.0005). Photos were taken at 3 dpi **(C)**, and bacterial growth was measured at 0 and 3 dpi **(D)**. Values are means ± SD, $^{**}P \leq 0.01$, $n = 3$.

(E) and **(F)** Pathogen/PAMP-triggered stomatal closure is dependent on MPK3/MPK6. Epidermal peels of Col-0, *MPK6SR* (line #58), and *MPK3SR* (line #64) plants were floated on stomatal opening buffer containing DMSO or NA-PP1 (2 μM) under light for 2.5 h and then exposed to flg22 for 3 h **(E)** or *Pst* (OD = 0.1) for 1 h **(F)** before stomatal aperture measurements. Values are means ± SD, $^{**}P \leq 0.01$, $n \geq 30$.

MKK4/MKK5 RNAi lines due to the partial knockdown nature of *mkk4* in this double mutant (Zhao et al., 2014). After being normalized to the stomatal density, the calculated pathogen entry rate of *mkk4 mkk5* double mutant was still significantly higher than that of the wild type (Figure 3H).

Based on gain-of-function evidence, it was concluded that MKK4/MKK5 function as redundant MAPKKs upstream of MPK3/MPK6 in plant immunity (Asai et al., 2002; Ren et al., 2002, 2008; Tsuda et al., 2013; Guan et al., 2015). With the available *mkk4 mkk5* double mutant, we were able to gain loss-of-function evidence to support the idea that MKK4/MKK5 are indeed upstream of MPK3/MPK6 in plant immune response. As shown in Figure 3I, flg22-induced MPK3/MPK6 activation was impaired in *mkk4 mkk5* double mutant (Figure 3I). There was a compensatory increase in MPK4 activation, similar to the *mpk3 mpk6* double mutant inoculated with *Botrytis cinerea* (Ren et al., 2008). Based on these results, we conclude that MKK4/MKK5, similar to their downstream kinases MPK3/MPK6, are essential to stomatal immunity. Furthermore, *mkk4 mkk5* double mutants were also more susceptible to infiltration-inoculated *Pst* (Figures 3J and 3K). In contrast, no change in pathogen growth was observed in *mkk4* and *mkk5* single mutants when *Pst* was either spray- or infiltration-inoculated (Supplemental Figures 7A and 7B). Furthermore, stomatal closure in response to flg22 treatment and pathogen entry remained the same in *mkk4* and *mkk5* single mutants (Supplemental Figures 7C and 7D), demonstrating that MKK4 and MKK5 function redundantly in stomatal immunity. It was previously reported that *MKK4*- or *MKK5*-overexpressing lines have

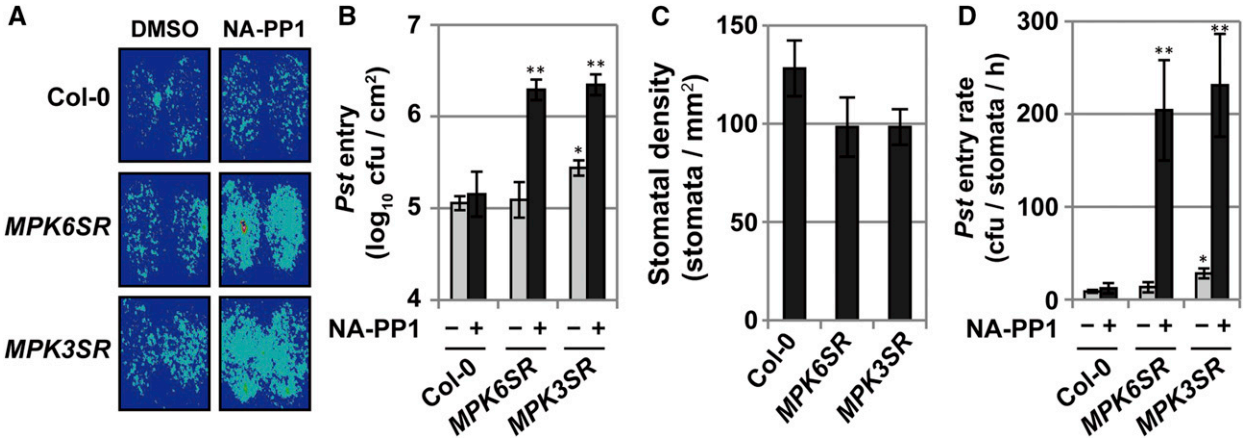

Figure 2. Pathogen Entry Assay Revealed a Compromised Stomatal Immunity in the *mpk3 mpk6* Double Mutant.

(A) and **(B)** Detached leaves of Col-0, *MPK6SR* (line #58), and *MPK3SR* (line #64) plants were floated on stomatal opening buffer containing DMSO or NA-PP1 (2 μM) under light for 2.5 h and then exposed to *Pst-lux* (OD = 0.5) for 1 h. Leaves were washed with 0.02% Silwet L-77 with stirring. *Pst* entry was measured by photon counting imaging **(A)** or direct counting of the bacterial population **(B)**. Values are means ± SD, *P ≤ 0.05 and **P ≤ 0.01, $n = 3$.
(C) Stomatal density was determined using leaves of the same position from Col-0, *MPK6SR* (line #58), and *MPK3SR* (line #64) plants. Values are means ± SD, $n = 6$.
(D) *Pst* entry rates were calculated as *Pst* number per mm^2 divided by stomatal density (number of stomata per mm^2) in 1 h. Values are means ± SD, *P ≤ 0.05 and **P ≤ 0.01, $n = 3$.

enhanced resistance against powdery mildew *Golovinomyces cichoracearum* (Zhao et al., 2014). However, no change in apoplastic or stomatal immunity against *Pst* was observed in these *MKK4*- or *MKK5*-overexpressing lines (Supplemental Figures 7A to 7D), possibly due to differential defense mechanisms against *Pst* and powdery mildew in Arabidopsis. Taking these results together, we can conclude that the MKK4/MKK5-MPK3/MPK6 module plays essential roles in both stomatal and apoplastic immunity against *Pst*. In this study, we mainly focus on the role of this signaling module in stomatal immunity.

MPK3/MPK6 Activation-Induced Stomatal Closure Is Independent of ABA Biosynthesis and Signaling

Using conditional gain-of-function *GVG*-Nt-*MEK2*^{DD} transgenic Arabidopsis (abbreviated as *DD*) (Ren et al., 2002), we found that activation of MPK3/MPK6 in *DD* plants after dexamethasone (DEX) treatment was sufficient to induce stomatal closure (Figure 4A), which supports our conclusion based on loss-of-function analyses. DEX itself had no effect on stomatal behavior in Col-0 plants (Figure 4A), demonstrating that DEX-induced stomatal closure in *DD* plants was a result of MPK3/MPK6 activation. To test whether the gain-of-function MPK3/MPK6 activation-induced stomatal closure is dependent on ABA, we crossed *DD* with mutants of ABA biosynthesis (*aba2-1*) (González-Guzmán et al., 2002) and signaling (*abi1-11* and *ost1-3*) (Hua et al., 2012; Acharya et al., 2013) as well as downstream components in stomatal closure (*slac1-3* and *rbohD*) (Torres et al., 2002; Negi et al., 2008; Vahisalu et al., 2008). F3 double homozygous lines were used for stomatal closure assay. We found that MPK3/MPK6 activation-induced stomatal closure was normal in the absence of ABA biosynthesis or signaling (Figures 4B and 4C), demonstrating that MPK3/MPK6 activation induces stomatal closure through a pathway independent of ABA biosynthesis and signaling. Moreover, MPK3/MPK6 activation-induced stomatal closure is independent of SLAC1. In addition, ABA treatment could induce stomatal closure in *MPK3SR* and *MPK6SR* plants with and without NA-PP1 pretreatment and in the *mkk4 mkk5* double mutant (Supplemental Figures 8A to 8C), suggesting again that ABA and MPK3/MPK6 are independent of each other in inducing stomatal closure. Interestingly, MPK3/MPK6 activation induces stomatal closure is more pronounced in *aba2-1* and *abi1-11* background (Figure 4B). In addition, stomatal closure induced by ABA treatment is more pronounced in NA-PP1-treated *MPK3SR* and *MPK6SR* plants and *mkk4 mkk5* double mutant (Supplemental Figures 8B and 8C). It is possible that both MAPK and ABA signaling pathways are essential for stomatal regulation. In the absence of one pathway, there is a compensatory enhancement in the sensitivity of the other pathway. Alternatively, these two pathways may negatively regulate each other's activity to fine-tune stomatal aperture in response to changing environmental conditions. Future studies are needed to determine the possible link between these two pathways.

MPK3/MPK6 Activation-Induced Stomatal Closure Is Related to Malate/Citrate Metabolism

To explore whether MPK3/MPK6 activation-induced stomatal closure is related to metabolic conversion of osmotically active molecules, such as sucrose, malate, and citrate, we examined starch accumulation and malate/citrate metabolism in guard cells after MPK3/MPK6 activation. As shown in Supplemental Figure 9, starch accumulation in guard cells was comparable in ethanol (solvent control) and DEX-treated *DD* plants. Interestingly, MPK3/MPK6 activation-induced stomatal closure was strongly impaired in the presence of malate or citrate (Figure 4D). Next, we checked

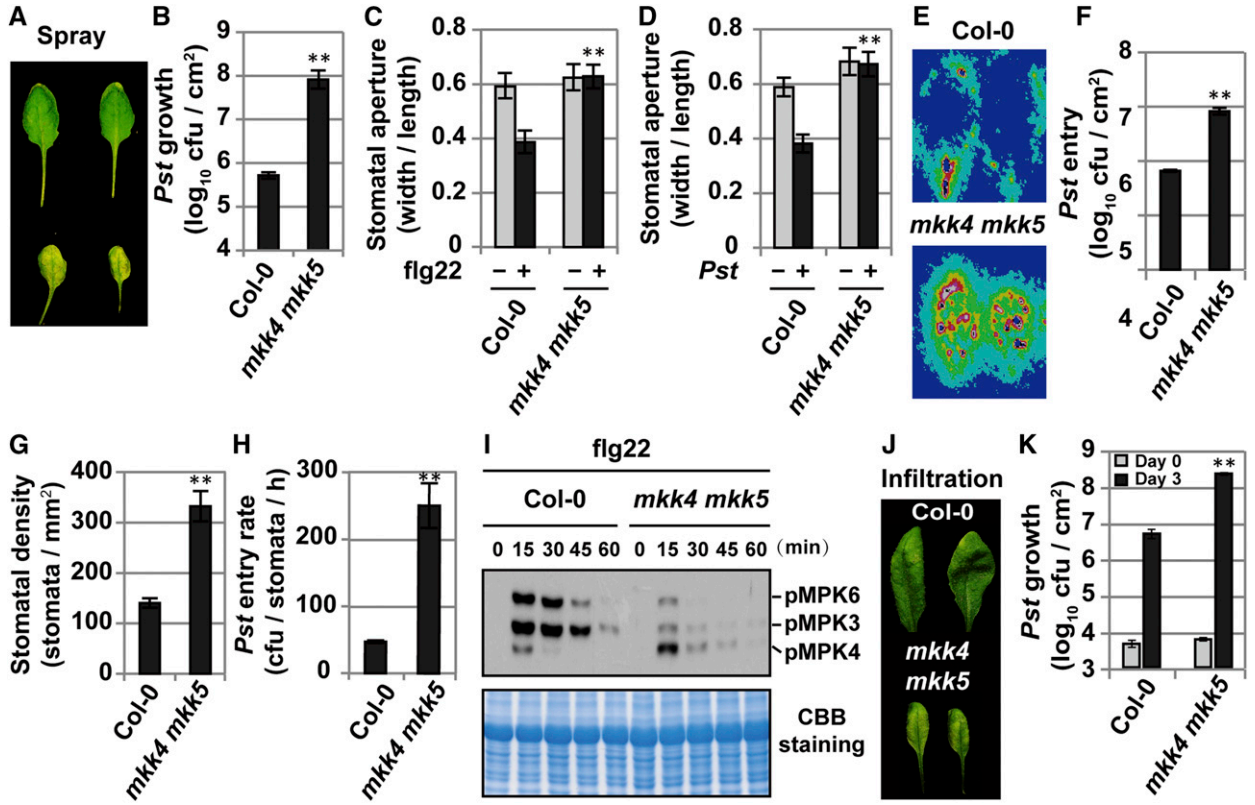

Figure 3. *MKK4* and *MKK5* Play a Redundant Role in Stomatal Immunity.

(A) and **(B)** Loss of function of *MKK4* and *MKK5* compromises plant resistance against *Pst*. Col-0 and *mkk4 mkk5* double mutant plants were spray-inoculated with *Pst* (OD = 0.5). Photos were taken at 3 dpi **(A)** and bacterial growth was measured at 2.5 dpi **(B)**. Values are means ± SD, **P ≤ 0.01, $n = 3$.

(C) and **(D)** Pathogen/PAMP-induced stomatal closure is dependent on MKK4/MKK5. Leaves of Col-0 and *mkk4 mkk5* plants were floated on stomatal opening buffer under light for 2.5 h and then exposed to flg22 for 3 h **(C)** or *Pst* (OD = 0.1) for 2 h **(D)** before stomatal aperture was measured. Values are means ± SD, **P ≤ 0.01, $n \geq 30$.

(E) and **(F)** Pathogen entry assay revealed a compromised stomatal immunity in the *mkk4 mkk5* double mutant. Detached leaves of Col-0 and *mkk4 mkk5* plants were floated on stomatal opening buffer under light for 2.5 h and then exposed to *Pst-lux* (OD = 0.5) for 1 h. Leaves were washed in 0.02% Silwet L-77 with stirring. *Pst* entry was measured by photon counting **(E)** or direct counting of the bacterial population **(F)**. Values are means ± SD, **P ≤ 0.01, $n = 3$.

(G) Increased stomatal density of *mkk4 mkk5* double mutant. Values are means ± SD, **P ≤ 0.01, $n = 6$.

(H) *Pst* entry rate was calculated by dividing *Pst* number per mm^2 by stomatal density. Values are means ± SD, **P ≤ 0.01, $n = 3$. Note: For measuring stomatal aperture in *mkk4 mkk5*, only separated stomata were selected for analysis.

(I) Loss of function of MKK4 and MKK5 compromises flg22-induced MPK3/MPK6 activation. Twelve-day-old Col-0 and *mkk4 mkk5* seedlings grown in liquid 0.5× Murashige and Skoog medium were treated with 50 nM flg22 for the indicated time. MAPK activation was detected by immunoblot analysis using anti-pTEpY antibody. Equal loading was confirmed by Coomassie blue (CBB) staining.

(J) and **(K)** Loss of function of MKK4 and MKK5 compromises apoplastic immunity. Col-0 and *mkk4 mkk5* plants were infiltration-inoculated with *Pst* (OD_{600} = 0.0005). Photos were taken at 3 dpi **(J)**, and bacterial growth was measured at 0 and 3 dpi **(K)**. Values are means ± SD, **P ≤ 0.01, $n = 3$.

the expression of several genes encoding enzymes in organic acid metabolism. As shown in Figure 4E, MPK3/MPK6 activation increased the expression of genes encoding NAD-isocitrate dehydrogenase 1 (NAD-IDH1), NAD-IDH2, NAD-IDH5, NADP-malate enzyme 2 (NADP-ME2), and NADP-ME3, while the expression of genes encoding NADP-ME4, NAD-malate enzyme 2 (NAD-ME1), and NAD-ME2 was not affected. Associated with the activation of genes encoding enzymes involved in malate metabolism, we detected a decrease in cellular malate contents in whole leaves (Supplemental Figure 10A).

The above experiments were done using whole leaves because wounding associated with guard cell protoplast isolation will activate MPK3/MPK6, which will complicate the results. In silico analysis revealed that genes encoding enzymes in malate metabolism and the TCA cycle are expressed at comparable levels in guard cells and whole leaves (Supplemental Table 1). To gain more direct evidence, we examined the enzyme activities in guard cells using in situ enzyme activity staining (Baud and Graham, 2006). The activity of NAD-ME, NADP-ME, NAD-IDH, and NADP-IDH all increased upon MPK3/MPK6 activation, among them the increase in NADP-ME and NAD-IDH activities were much higher compared with the others (Figure 4F; Supplemental Figure 11). These results suggest that MPK3/MPK6 activation-induced stomatal closure might involve metabolic conversion of osmotically active organic acids.

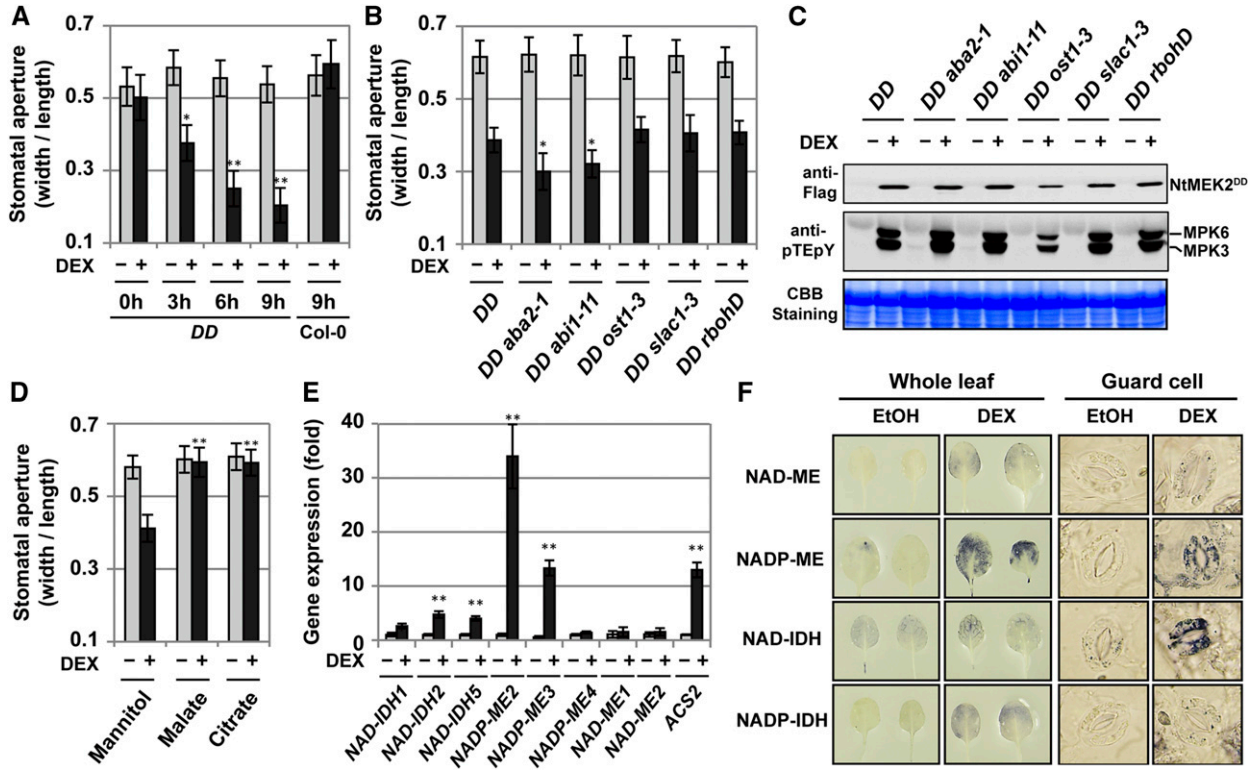

Figure 4. MPK3/MPK6 Activation-Induced Stomatal Closure Is Independent of ABA but Related to Organic Acid Metabolism.

(A) Gain-of-function activation of MPK3/MPK6 induces stomatal closure. Epidermal peels of *DD* and Col-0 plants were floated on stomatal opening buffer under light for 2.5 h and then treated with DEX (5 μM) or ethanol (solvent of DEX stock solution). Stomatal aperture was determined at indicated time after DEX treatment. Values are means ± SD, *P ≤ 0.05 and **P ≤ 0.01, $n \geq 30$.

(B) MPK3/MPK6 activation is sufficient to triggered stomatal closure in the absence of ABA biosynthesis or signaling. Detached leaves from *DD*, *DD aba2-1*, *DD abi1-11*, *DD ost1-3*, *DD slac1-3*, and *DD rbohD* plants were floated on stomatal opening buffer under light for 2.5 h and then treated with ethanol or DEX (5 μM) for 5 h before stomatal aperture was determined. Values are means ± SD, *P ≤ 0.05, $n \geq 30$.

(C) DD induction and MPK3/MPK6 activation in *DD*, *DD aba2-1*, *DD abi1-11*, *DD ost1-3*, *DD slac1-3*, and *DD rbohD* plants. Leaf tissues were collected at the time of aperture measurement as in **(B)**. Induction of *DD* expression and MPK3/MPK6 activation were detected by immunoblot analysis using anti-Flag and anti-pTEpY antibodies, respectively. Equal loading was confirmed by Coomassie blue (CBB) staining.

(D) Exogenously added malate or citrate can reverse MPK3/MPK6-induced stomatal closure. *DD* plants were first dark-adapted for 1 h. Detached leaves were floated on stomatal opening buffer containing mannitol, malate, or citrate (20 mM) under light for 2.5 h and then treated with ethanol or DEX (5 μM) for 5 h before stomatal aperture was measured. Values are means ± SD, **P ≤ 0.01, $n \geq 30$.

(E) Induction of genes encoding enzymes in organic acid metabolism. Total RNA was extracted from 3-week-old *DD* plants treated as in **(B)**. Transcript levels were determined by quantitative RT-PCR. *EF1α* was used as an internal control. Values are means ± SD, **P ≤ 0.01, $n = 3$.

(F) In situ enzyme activity assays revealed an increase in malate/citrate metabolic enzymes in guard cells after MPK3/MPK6 activation. *DD* plants were treated as in **(B)**, and the in situ enzyme activity assay was performed as described.

Pathogen/PAMP-Induced NADP-ME and NAD-IDH Activities Are Dependent on MKK4/MKK5-MPK3/MPK6

Gain-of-function evidence revealed that MPK3/MPK6 activation could enhance the activities of enzymes involved in malate metabolism in guard cells. We next tested whether pathogen/PAMPs could also increase the gene expression and activity of these enzymes. As shown in Supplemental Figures 12A and 12B, *NADP-ME2* expression was induced after flg22 treatment or *Pst* inoculation. For the enzyme activity staining, we mainly focused on NADP-ME and NAD-IDH because their high induction by MPK3/MPK6 activation. As shown in Figure 5, enzymatic activities of NADP-ME and NAD-IDH were highly induced by flg22 or *Pst* in wild-type plants, which is again associated with a decrease in cellular malate contents in whole leaves (Supplemental Figures 10B and 10C).

To gain loss-of-function evidence to support the role of MKK4/MKK5-MPK3/MPK6 module in regulating malate metabolism, we analyzed the NADP-ME and NAD-IDH activities in *mkk4 mkk5* and the conditional *mpk3 mpk6* double mutants. To our surprise, the basal activities of NADP-ME and NAD-IDH were substantially higher in untreated *mkk4 mkk5* double mutant (Figure 5). After treatment with flg22 or *Pst*, the activity of NADP-ME and NAD-IDH did not increase; instead, we observed a slight decrease in their activities (Figure 5). Furthermore, we found that the basal activities of NADP-ME were also

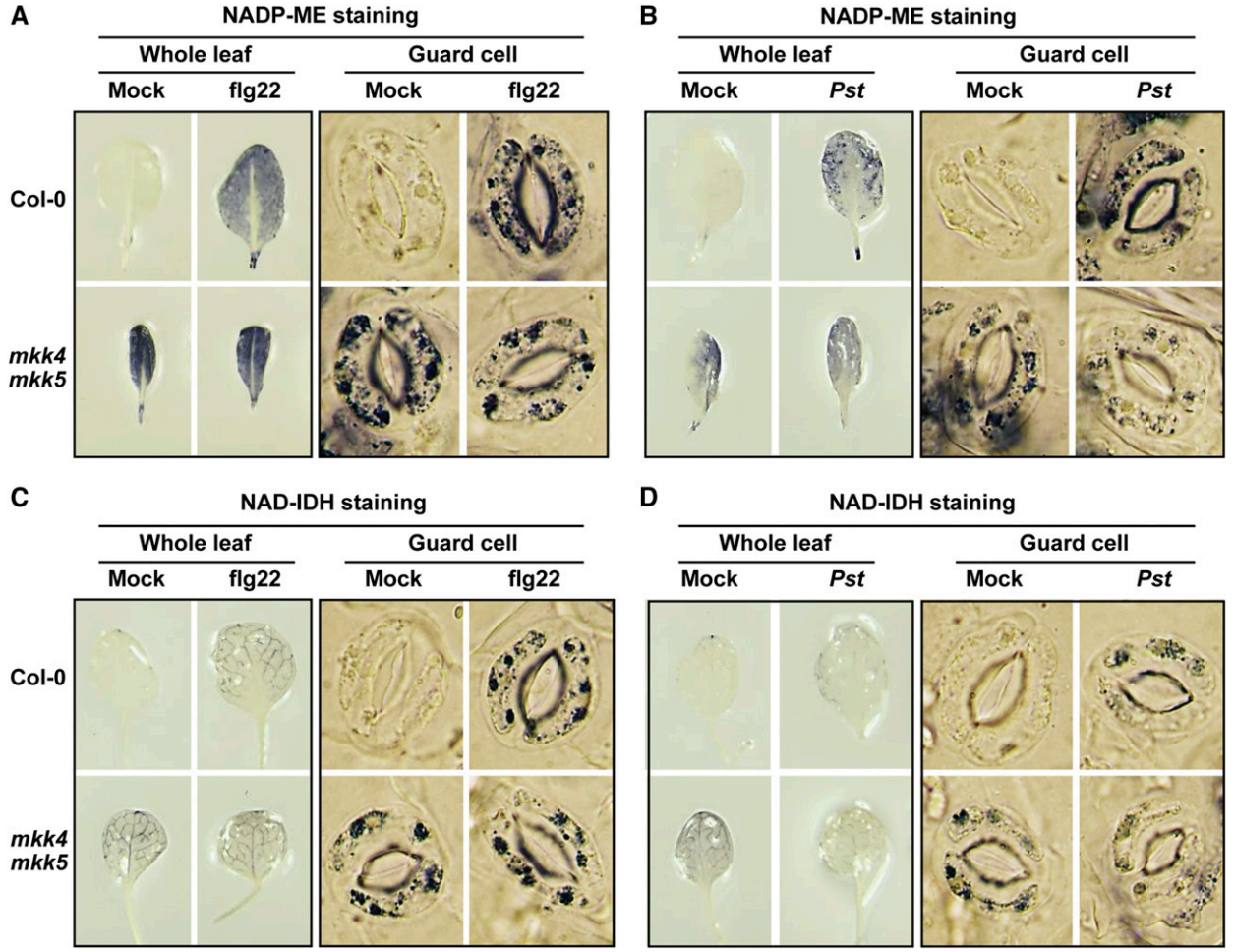

Figure 5. *MKK4* and *MKK5* Are Required for flg22- or *Pst*-Induced Activation of NADP-ME and NAD-IDH.

Intact leaves of Col-0 and *mkk4 mkk5* plants were floated on stomatal opening buffer under light for 2.5 h and then exposed to flg22 for 3 h (**[A]** and **[C]**) or *Pst* (OD = 0.1) for 2 h (**[B]** and **[D]**). After being fixed in paraformaldehyde solution for 1 h, and washed overnight, the leaves were subjected to in situ NADP-ME (**[A]** and **[B]**) or NAD-IDH (**[C]** and **[D]**) activity staining.

higher in NA-PP1-treated, but not in DMSO-treated, *MPK3SR* and *MPK6SR* plants (Supplemental Figure 13). Similar with that in *mkk4 mkk5* double mutant, activity of NADP-ME in NA-PP1-treated *MPK3SR* and *MPK6SR* plants failed to increase after *Pst* inoculation; instead, we observed a decrease in NADP-ME activity. These results demonstrated that the MKK4/MKK5-MPK3/MPK6 module is required for pathogen/PAMP-induced increase in organic acid metabolism in guard cells as indicated by the increase in enzymatic activities, and loss of function of MKK4/MKK5-MPK3/MPK6 signaling also affects the basal level activities of these enzymes.

Stomatal Immunity Is Impaired in the Presence of Malate or Citrate

The results above support a notion that metabolic conversion of osmotically active organic acids plays a role in stomatal immunity. To provide further evidence, we performed pathogen entry assay in leaves treated with malate or citrate. Mannitol was included as a control. There was a large increase in *Pst-lux* entry in the presence of malate or citrate (Figures 6A and 6B), which was accompanied by the impairment of *Pst*-induced stomatal closure (Figure 6C). In contrast, the nonmetabolizable mannitol did not have these effects. These results further support the importance of metabolic conversion of osmotically active organic acids in stomatal immunity.

A recent study showed that plant-secreted bioactive metabolites including malate and citrate could stimulate the expression of type III effectors and therefore enhance the pathogen virulence (Anderson et al., 2014). To test whether the impaired stomatal immunity is a result of enhanced virulence of *Pst* in the presence of malate or citrate, we first treated *Pst-lux* with mannitol, malate, or citrate for 1 h and then performed pathogen entry assay using these pretreated *Pst-lux*. As shown in Figures 6D and 6E, *Pst-lux* entry into leaves was not affected.

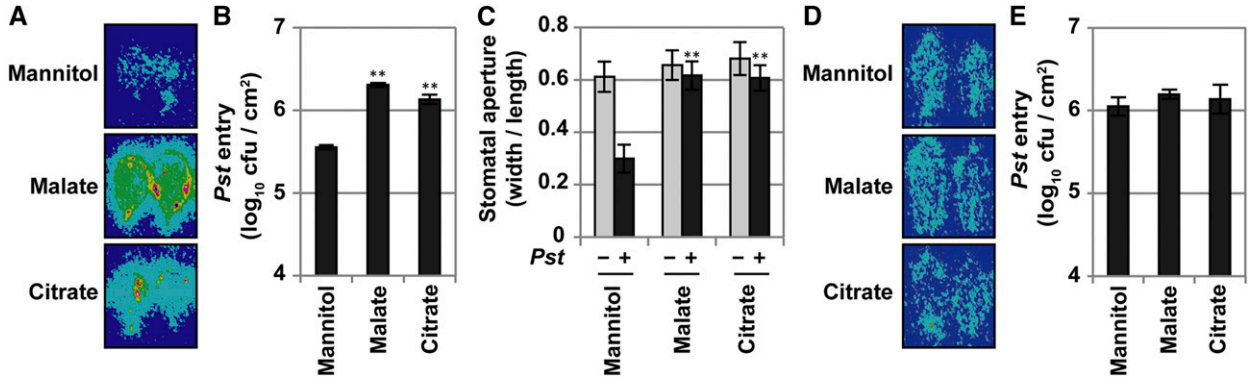

Figure 6. Stomatal Immunity Is Impaired in the Presence of Malate or Citrate.

(A) and **(B)** Pathogen entry assay demonstrated that treatment with malate or citrate reduces stomatal immunity. Plants were first dark-adapted for 1 h. Detached leaves were floated on stomatal opening buffer containing mannitol, malate, or citrate (20 mM) under light for 2.5 h, and then exposed to *Pst-lux* (OD_{600} = 0.5) for 1 h. After washing, *Pst* entry was measured by photon counting **(A)** or by direct counting of the bacterial population **(B)**. Values are means ± SD. **P ≤ 0.01, n = 3.

(C) Pathogen-induced stomatal closure is impaired by malate or citrate. Plants were first dark-adapted for 1 h. Detached leaves were floated on stomatal opening buffer containing mannitol, malate, or citrate under light for 2.5 h and then exposed to *Pst-lux* (OD_{600} = 0.1) for 2 h. Values are means ± SD, **P ≤ 0.01, $n \geq 30$.

(D) and **(E)** Compromised stomatal immunity by malate or citrate treatment is not related to induced pathogen virulence. *Pst-lux* was first suspended in stomatal opening buffer containing mannitol, malate, or citrate for 1 h and washed twice with stomatal opening buffer. These pretreated *Pst-lux* bacteria were then used for inoculation. *Pst* entry was measured by photon counting **(D)** or by direct counting of the bacterial population **(E)**. Values are means ± SD, n = 3.

Differential Sensitivity of ABA- and MPK3/MPK6-Induced Stomatal Closure to Coronatine

The essential function of ABA in plant stomatal defense, as suggested in a number of reports (Melotto et al., 2006; Zeng and He, 2010; Du et al., 2014; Lim et al., 2014), was recently called into question (Montillet et al., 2013). Thus, we reexamined the importance of ABA biosynthesis and signaling in stomatal immunity using the pathogen entry assay. As shown in Figures 7A and 7B, *Pst-lux* entry was much higher in *aba2-1*, *ost1-3*, *slac1-3*, and *rbohD* mutants. In addition, flg22- or *Pst*-induced stomatal closure was strongly impaired in *aba2-1*, *ost1-3*, *slac1-3*, and *rbohD* (Figures 7C and 7D), supporting the conclusion that ABA biosynthesis and signaling are essential to stomatal immunity.

COR, a phytotoxin produced by *Pst*, is able to open plant stomata to facilitate the pathogenesis process (Melotto et al., 2006; Zheng et al., 2012). Consistent with previous reports, ABA-induced stomatal closure could be blocked by COR (Figure 8A). However, MPK3/MPK6 activation-induced stomatal closure was insensitive to COR (Figure 8B). In addition, we found that activities of NADP-ME and NAD-IDH were not induced by ABA (Supplemental Figure 14), indicating that ABA-induced stomatal closure is independent of metabolic conversion of osmotically active organic acids. Furthermore, we found that MPK3/MPK6 activation-induced stomatal closure could not be reopened by *Pst* (Figures 8C and 8D). These observations further support that ABA and MKK4/MKK5-MPK3/MPK6 represent two different pathways in mediating stomatal closure.

DISCUSSION

In this study, we demonstrate that Arabidopsis MPK3 and MPK6 are essential to plant immunity. They play redundant functions in both stomatal and apoplastic immunity. MKK4 and MKK5 are redundant MAPKKs upstream of MPK3 and MPK6 in the same pathway based on genetic and biochemical analyses. Stomatal aperture measurements and pathogen entry assays revealed that *mpk3 mpk6* and *mkk4 mkk5* double mutants were unable to close their stomata in response to PAMP treatment or *Pst* inoculation, which leads to compromised resistance in these mutants (Figures 1 to 3). It appears that MPK3/MPK6 activation promotes the metabolic conversion or consumption of osmotically active organic acids and therefore induces stomatal closure during plant defense responses. Furthermore, we found that MPK3/MPK6-induced stomatal closure is independent of ABA biosynthesis and signaling (Figures 4A to 4C), despite the fact that ABA is essential to stomatal immunity (Figures 7A to 7D) (Melotto et al., 2006; Zheng et al., 2012; Du et al., 2014). We proposed an interdependent model in which the MPK3/MPK6 pathway and the ABA pathway can independently trigger stomatal closure when MPK3/MPK6 are activated in the gain-of-function system or when ABA is exogenously applied, but both pathways are required for an effective stomatal immunity upon sensing of pathogen PAMPs (Figure 8E).

Previous studies showed that *mpk3* and *mpk6* single mutants as well as guard cell-specific *MPK3* antisense plants were strongly impaired in flg22-, bacterium-, or LPS-induced stomatal closure (Gudesblat et al., 2009; Montillet et al., 2013). It was also reported that ABA-dependent and ABA-independent (but MPK3- or MPK6-dependent) pathways converge on SLAC1 in stomatal immunity (Montillet et al., 2013). Our gain-of-function data showed that MAPK activation-induced stomatal closure is independent of SLAC1 (Figure 4B), but related to organic acids metabolism (Figures 4D to 4F). More importantly, no clear susceptible phenotype was observed in *mpk3* single mutant, and only a slightly

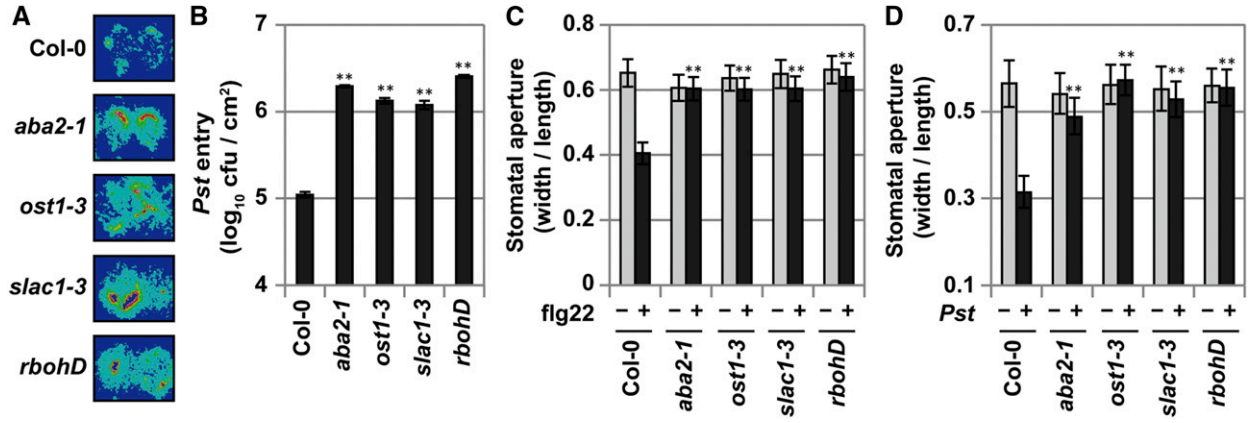

Figure 7. ABA Signaling Is Essential to Stomatal Immunity.

(A) and **(B)** Elevated pathogen entry in ABA biosynthesis and signaling mutants. Intact leaves of Col-0, *aba2-1*, *ost1-3*, *slac1-3*, and *rbohD* plants were floated on stomatal opening buffer under light for 2.5 h and then exposed to *Pst-lux* (OD_{600} = 0.5) for 1 h. *Pst* entry was measured by photon counting **(A)** or by direct counting of the bacterial population **(B)**. Values are means ± SD, **P ≤ 0.01, n = 3.

(C) and **(D)** Pathogen/PAMP-induced stomatal closure is dependent on ABA biosynthesis and signaling. Intact leaves of Col-0, *aba2-1*, *ost1-3*, *slac1-3*, and *rbohD* plants were floated on stomatal opening buffer under light for 2.5 h and then exposed to flg22 for 3 h **(C)** or *Pst* (OD_{600} = 0.1) for 2 h **(D)**. Values are means ± SD, **P ≤ 0.01, $n \geq 30$.

higher bacterial growth was observed in the *mpk6* mutant (0.01< P < 0.05) when spray- or infiltration-inoculated with *Pst* (Supplemental Figures 1A and 1C), which is not consistent with the reported deficiency in stomatal immunity in the *mpk3* and *mpk6* single mutants. Furthermore, our detailed analysis revealed that *mpk3* and *mpk6* single mutants exhibited normal flg22-induced stomatal closure (Supplemental Figure 1B). It is possible that the inconsistency is a result of the weak phenotype of the single MAPK mutant/RNAi lines and the variation of assay conditions. In contrast, the double *mpk3 mpk6* and *mkk4 mkk5* mutant plants showed consistent and strong phenotypes that could be easily observed.

In our model, the MKK4/MKK5-MPK3/MPK6 pathway and ABA pathway function interdependently. Instead of converging on SLAC1, they modulate two different facets of osmoregulation in guard cells during pathogen/PAMP-induced stomatal closure. Activation of ABA signaling pathway leads to the activation of OST1 kinase that can directly phosphorylate RbohD and SLAC1, resulting in efflux of inorganic anions (mainly Cl^-) through SLAC1 (Negi et al., 2008; Vahisalu et al., 2008; Geiger et al., 2009) and cause subsequent plasma membrane depolarization, activation of quick anion channel (QUAC1) (Sasaki et al., 2010), and outward recertifying K^+ channel (Hosy et al., 2003). In contrast, activation of MPK3/MPK6 cascade stimulates metabolic conversion of osmotically active organic acids. Together, these two pathways would confer robust stomatal immunity. Interdependent regulation appears to be a common strategy to confer signaling robustness. A recent study demonstrated that SLAC1 activity was also interdependently regulated by OST1 and CDPKs, in which phosphorylation of SLAC1 at Ser-59 and Ser-120 by OST1 and CDPKs, respectively, are both essential for ABA-induced stomatal closure (Brandt et al., 2015).

ABA and MPK3/MPK6 pathways also differ in their sensitivity to COR, a phytotoxin. The ABA signaling pathway can be blocked by COR (Figure 8A), as reported (Zheng et al., 2012). In contrast, the MPK3/MPK6 activation-mediated stomatal closure is insensitive to COR (Figure 8B). It is worth noting that MPK3/MPK6 activation in the conditional gain-of-function *DD* system is longer lasting or higher in magnitude than that after flg22 treatment or *Pst* infection (Figure 3I) (Ren et al., 2002; Guan et al., 2015). Instead, it is similar to MPK3/MPK6 activation in plants after necrotrophic fungal infection or during effector-triggered immunity in duration and magnitude (Ren et al., 2008; Tsuda et al., 2013), implying a possible role for this stronger and longer lasting MPK3/MPK6 activation in necrotrophic fungal infection- or effector-triggered immunity-related stomatal immunity. It was reported previously that MPK9 and MPK12 function downstream of ROS and modulate SLAC1 activity in guard cell ABA signaling (Jammes et al., 2009, 2011). Based on genetic and biochemical analyses, MKK4 and MKK5 are unable to activate MPK9 and MPK12 in vivo and in vitro (Asai et al., 2002; Lee et al., 2009; Nagy et al., 2015). As a result, MPK9/MPK12 and MPK3/MPK6 are likely to function as two independent MAPK cascades in stomatal movement. In our model, we emphasized the potential role of MPK3/MPK6 in promoting the metabolism of malate/citrate. However, we currently cannot exclude the possibility that the transportation of these organic acids in and out of cells and/or vacuoles is also regulated in the process.

AtABCB14, an ABC transporter, was identified as a plasma membrane-localized malate importer to modulate stomatal movement in response to CO_2 (Lee et al., 2008). The plasma membrane-localized malate exporter, aluminum-activated malate transporter 12 (ALMT12), was shown to be involved in ABA- and CO_2-induced stomatal closure (Meyer et al., 2010). In addition, γ-aminobutyric acid can control the transporter activity of ALMTs (Ramesh et al., 2015; Gilliham and Tyerman, 2016). At this stage, the role of ALMTs in pathogen- and/or PAMP-mediated stomatal closure remains to be determined. Recently, starch biosynthesis

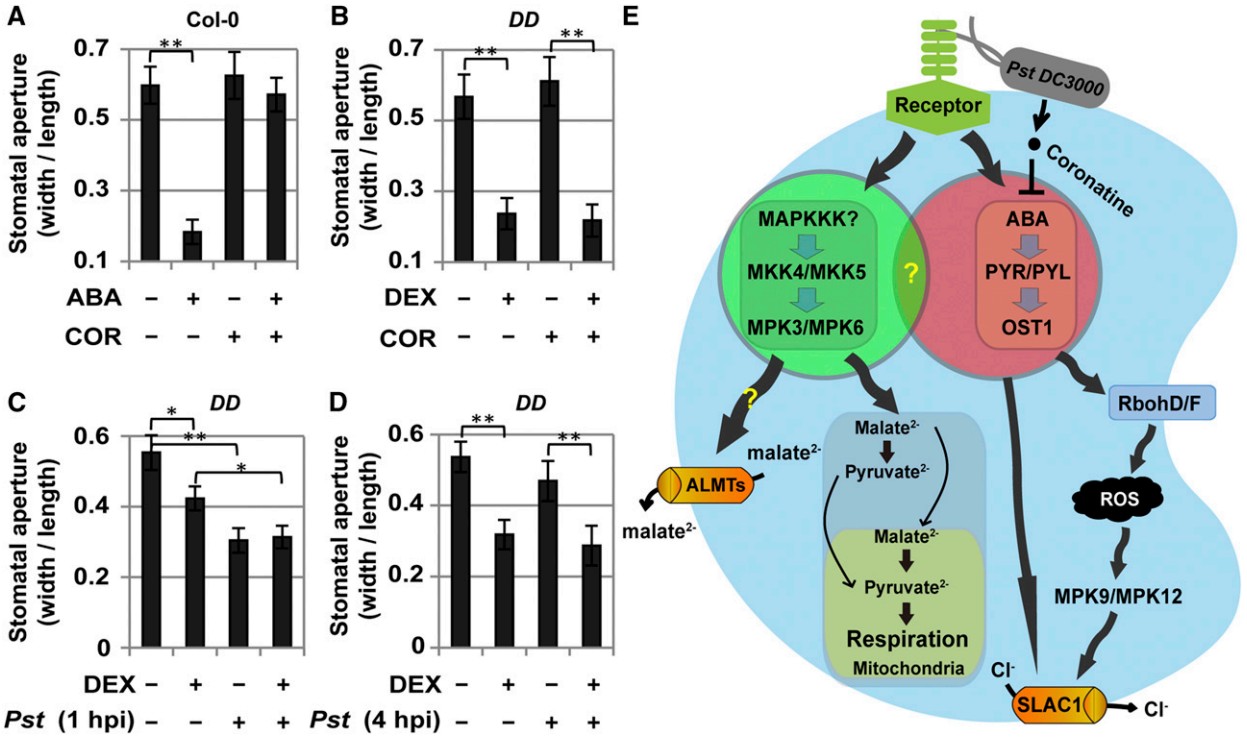

Figure 8. MPK3/MPK6 Activation-Induced Stomatal Closure Is Insensitive to Coronatine.

(A) ABA-induced stomatal closure is sensitive to coronatine. Intact leaves of Col-0 plants were floated on stomatal opening buffer under light for 2.5 h and then treated with ethanol (solvent control), ABA (10 μM), or COR (1 μg/mL). Stomatal aperture was measured 3 h later.
(B) Gain-of-function MPK3/MPK6 activation-induced stomatal closure is insensitive to coronatine. Intact leaves of *DD* plants were floated on stomatal opening buffer under light for 2.5 h and then treated with ethanol (solvent control), DEX (5 μM), or COR (1 μg/mL). Stomatal aperture was measured 5 h later.
(C) and **(D)** Gain-of-function activation of MPK3/MPK6 abolishes pathogen-induced stomatal reopening. Intact leaves of *DD* plants were floated on stomatal opening buffer under light for 2.5 h and then treated with ethanol or DEX (5 μM) for 3 h, which was followed by treatment with *Pst* for another 1 h **(C)** or 4 h **(D)**. In **(A)** to **(D)**, values are means ± SD, *P ≤ 0.05 and **P ≤ 0.01, $n \geq 30$.
(E) MPK3/MPK6 cascade and ABA function interdependently to regulate stomatal immunity. In this model, pathogen-responsive MPK3/MPK6 cascade and ABA are both required for stomatal immunity. Upon perception of pathogen/PAMPs, both pathways are activated. Activation of MPK3/MPK6 by MKK4/MKK5 increases malate/citrate metabolism, which leads to a decrease in malate/citrate content. ABA signaling pathway activates OST1, which can directly phosphorylate RbohD and SLAC1 and activate SLAC1-mediated Cl^- efflux, which leads to plasma depolarization and subsequent K^+ efflux. Different from the MPK3/MPK6 cascade, MPK9 and MPK12, two guard cell-specific MAPKs, are involved in SLAC1 activation and stomatal closure in response to ABA and ROS. COR inhibits ABA-mediated but not MPK3/MPK6 cascade-mediated stomatal closure.

was implicated in high CO_2-induced stomatal closure (Azoulay-Shemer et al., 2016). However, Lugol's IKI staining indicated no change in starch accumulation after MPK3/MPK6 activation (Supplemental Figure 9), suggesting that starch biosynthesis may not play any role in PAMP/pathogen-induced stomatal closure.

At this point, measuring the change in malate or citrate levels in guard cells in response to MPK3/MPK6 activation during plant immunity remains technically challenging. We attempted to enrich the epidermal fraction using the blender method (Zhang et al., 2008). In parallel, we also included a group with Cellulase R-10 and Macerozyme R-10 treatment to remove mesophyll cells attached to epidermal strips. In both case, we found malate levels were too low to be reliably detected in both ethanol- and DEX-treated *DD* samples. This could be a result of strong MPK3/MPK6 activation caused by the wounding stress and cell wall elicitor released during protoplast preparation, which in turn can activate the expression of genes encoding enzymes related to organic acid metabolism. Consistent with this, we observed that leaf petiole wounded by forceps during handling showed higher NADP-ME and NAD-IDH activities (Figure 4F; Supplemental Figures 11 and 13 to 15). (Note: We removed portions of the leaf petioles that had higher activity staining when possible before photography. As a result, not all leaf petioles showed higher activity staining.) Developing tools that will allow in situ single-cell detection such as cellular sensors of malate or citrate will be required to achieve this goal. Nonetheless, we found that malate content decreases in whole leaves after MPK3/MPK6 activation in *DD* plants (Supplemental Figure 10A) or Col-0 plants after pathogen/PAMP treatment (Supplemental Figures 10B and 10C). Furthermore, in situ enzyme activity assays revealed higher levels of increase in NADP-ME and NAD-IDH activities in guard cells than other types of leaf cells (Figures 4F and 5), which should correlate with a more pronounced decrease in malate in guard cells, supporting our working model (Figure 8E). In addition, we found that exogenously

added malate/citrate could block stomatal closure triggered by MPK3/MPK6 activation or *Pst* inoculation (Figures 4D and 6C) and compromise stomatal immunity (Figures 6A and 6B).

Due to gene redundancy and the nature of metabolic flexibility, it is very challenging to provide genetic evidence for the role of metabolic conversion of organic acids in stomatal immunity. There are four NADP-ME isoforms and two NAD-ME isoforms in Arabidopsis (Wheeler et al., 2005; Tronconi et al., 2008), and their function can be compensated for by each other. Although NADP-ME activity was greatly reduced in *nadp-me2* mutant, flg22-induced stomatal closure was not affected (Supplemental Figure 15). By using two independent *nadp-me2* alleles, a previous study also showed normal disease resistance against *Pst* (Wheeler et al., 2005; Li et al., 2013). Double mutant plants lacking both NAD-ME1 and NAD-ME2 also grow normally (Tronconi et al., 2008). Gene redundancy and functional compensation were also reported for NAD-IDH and NADP-IDH (Lemaitre et al., 2007; Mhamdi et al., 2010). Nonetheless, in our gain-of-function MPK3/MPK6 system, all four of these enzymes were activated (Figure 4F), and MPK3/MPK6 activation- and *Pst* inoculation-induced stomatal closure was impaired in the presence of malate or citrate (Figures 4D and 6C). Collectively, these results do support a positive role for metabolic conversion of organic acids in stomatal immunity.

MPK3/MPK6 activation results in an increase in the activities of NADP-ME and NAD-IDH in guard cells. Unexpectedly, we also observed higher basal-level activities of NADP-ME and NAD-IDH in the loss-of-function *mkk4 mkk5* double mutant (Figure 5). The basal-level activities of NADP-ME in NA-PP1-treated *MPK3SR* and *MPK6SR* plants were also higher than that of the control plants treated with DMSO (Supplemental Figures 13A and 13B), indicating that MKK4/MKK5-MPK3/MPK6 signaling module may also play a role in maintaining the basal levels of these enzymes in plants. It is possible that multiple signaling pathways are involved in controlling the activities of NADP-ME and NAD-IDH, which could be important in maintaining the metabolic homeostasis in plants. Loss of function of the MPK3/MPK6 cascade may result in the overcompensation as a result of the activation of the other signaling pathway. In mammals, both extracellular signal-regulated kinase 2 (ERK2; a MAPK) and cyclin-dependent kinase 5 (Cdk5) are involved in maintaining glucose homeostasis in adipose tissues by phosphorylating PPARγ (peroxisome proliferator-activated receptor γ) on Ser-273 (Choi et al., 2010). However, when Cdk5 is knocked out, PPARγ phosphorylation on the Ser-273 residue was found to be much higher. It turns out that, besides PPARγ, Cdk5 can also phosphorylate the MAPKK upstream of ERK2 on a novel site and inhibit ERK2 activation (Banks et al., 2015). The loss of Cdk5, therefore, leads to the hyperactivation of ERK2, resulting in a higher level of phosphorylation of PPARγ on Ser-273. It will be interesting to determine the signaling pathways that crosstalk with MKK4/MKK5-MPK3/MPK6 in maintaining the basal organic acid metabolism in guard cells.

During light-induced stomatal opening, tobacco guard cells were capable of fixing CO_2, operating the TCA cycle, and synthesizing amino acids (Daloso et al., 2015). Furthermore, the levels of TCA cycle intermediates and amino acids are dynamically regulated and respond differently to K^+ and sucrose, suggesting that guard cells may take advantage of the flexibility of metabolism to fine-tune stomatal aperture during stomatal opening. It was previously shown that *Sclerotinia sclerotiorum*, a phytopathogenic fungus, interferes with the stomatal immunity by secreting oxalate, an intermediate of the TCA cycle (Guimarães and Stotz, 2004). In addition, oxalate could promote stomatal opening and inhibit ABA-induced stomatal closure (Guimarães and Stotz, 2004). Citrate, another intermediate of the TCA cycle, could also promote stomatal opening and delay dark-induced stomatal closure (Jinno, 1981). It is worth noting that, in these two studies, oxalate or citrate was added to closed stomata. Upon illumination, oxalate or citrate is imported into guard cell and thus increases turgor pressure, which delays ABA- or dark-induced stomatal closure. In another study, it was found that malate or fumarate, both intermediates of the TCA cycle, induces stomatal closure when added to opened stomata (Araújo et al., 2011b). These TCA cycle intermediates may affect stomatal movement in two ways: (1) by functioning as osmolytes to open stomata (Lee et al., 2008), and (2) by functioning as signals to close the opened stomata (Araújo et al., 2011b). In a similar case, sucrose, as an osmolyte, accumulates gradually during the day to maintain stomatal in an open state (Lawson, 2009). However, exogenous application of sucrose to open stomata induces ABA signaling-dependent stomatal closure (Kelly et al., 2013).

In order to address the role of malate or citrate in MPK3/MPK6 activation- or *Pst*-induced stomatal closure, we first allowed the plants to dark-adapt for 1 h and then treated them with malate or citrate (Figures 4D and 6C). Under such conditions, both organic acids can block the stomatal closure induced by gain-of-function activation of MPK3/MPK6 or *Pst* inoculation. Together with previous studies, our data here highlight the importance of metabolic shift of organic acids such as malate and citrate in regulating stomatal movement. In plant immune response, the MPK3/MPK6 cascade and ABA are two essential and interdependent signaling pathways that control, respectively, organic acid metabolism and ion channels, two branches of osmotic regulation in guard cells that control stomatal opening/closure. The activation of both pathways would confer a robust response in plant stomatal immunity.

METHODS

Plant Materials and Growth Conditions

Arabidopsis thaliana plants were grown in soil under 10-h-day/14-h-night cycle at 22 °C in a Conviron walk-in growth chamber equipped with high intensity discharge lights. The light intensity was set to 100 μmol m^{-2} s^{-1}. The humidity of the growth chamber was set to 75% RH. Three- to four-week-old plants were used for experiments. Col-0 ecotype was used as the wild type. Mutant alleles and transgenic lines of *mpk3-1* (Salk_151594), *mpk6-2* (Salk_073907), *mpk6-3* (Salk_127507), *DD* (*GVG-NtMEK2^{DD}*), and *MPK6SR* (*mpk3 mpk6 P_{MPK6}:MPK6^{YG}*, lines # 31 and #58) were reported previously (Ren et al., 2002; Wang et al., 2007; Xu et al., 2014). *MPK3SR* (*mpk3 mpk6 P_{MPK3}:MPK3^{TG}*, lines #28 and #64) was generated similarly as *MPK6SR* (Xu et al., 2014). Thr-116 residue in the ATP binding pocket of MPK3 was mutated to Gly (MPK3^{TG}) in a genomic clone in pCambia3300 vector (www.cambia.org). *P_{MPK3}:MPK3^{TG}* construct was transformed into *mpk3 mpk6*/+ plants. Single-insertion lines with *MPK3^{TG}* expressed at a similar level as the endogenous *MPK3* were identified by immunoblot analysis using an anti-MPK3 antibody (Sigma-Aldrich). F3 homozygous *P_{MPK3}:MPK3^{TG}* transgenic plants in the *mpk3 mpk6* background (*mpk3 mpk6 P_{MPK3}:MPK3^{TG}*), also known as inhibitor-sensitized MPK3 variant-rescued plants (*MPK3SR*), line #64 was used in this study.

Mutant alleles of *nadp-me2-1* (Salk_073818), *aba2-1* (CS156), *ost1-3* (Salk_008068), *slac1-3* (Salk_099139), and *rbohD* (CS9555) were obtained from the Arabidopsis Biological Resource Center. The *abi1-11* mutant was kindly provided by Zhizhong Gong (China Agricultural University). The *mkk4* and *mkk5* single TILLING mutants (Zhao et al., 2014) were first backcrossed with Col-0 to remove the *er-105* mutant allele and then crossed to generate *mkk4 mkk5* double mutant. The MKK4- and MKK5-overexpressing lines, MKK4OE #5, MKK4OE #7, MKK5OE #2, and MKK5OE #5, were kindly provided by Dingzhong Tang (Chinese Academy of Sciences).

Pathogen Assay and Pathogen Entry Assay

For *Pst* resistance assay, 3- to 4-week-old Arabidopsis plants were spray-inoculated with *Pst* suspension (OD_{600} = 0.5) in 10 mM $MgCl_2$ with 0.02% Silwet L-77. The 5th and 6th leaves were detached and washed with 0.02% Silwet L-77 before leaf discs were punched out for bacterial growth assays as previously described (Guan et al., 2015).

For pathogen entry assays, detached leaves were first illuminated for 2.5 h to fully open stomata and then treated with *Pst-lux* (final OD = 0.5) for 1 h. The treated leaves were washed by 0.02% Silwet L-77 for 10 s with stirring at maximum setting. Pathogen entry was measured using a photon counting image system (Image 32 system; Photek) or by direct counting of colony-forming units.

In Situ Enzyme Activity Staining

In situ enzyme activity staining was performed as previously described with modifications (Baud and Graham, 2006). Leaves were fixed by vacuum infiltration in fixation solution (2% paraformaldehyde, 2% polyvinylpyrrolidone 40,000, and 1 mM DTT, pH = 7.0) for 1 h on ice. After fixation, the leaves were rinsed five times with distilled water and stored in water overnight at 4°C. For NAD-ME assay, the leaves were incubated in reaction solution (100 mM HEPES-KOH, pH 6.5, 4 mM nicotinamide adenine dinucleotide [NAD^+], 0.1 mM acetyl-CoA, 2 mM fructose-1,6-biphosphate, 2 mM fumarate, 5 mM $MnCl_2$, 5 mM malate, 0.8 mM nitroblue tetrazolium dye [NBT], and 0.4 mM phenazine methosulfate [PMS]) for 3 h at 30 °C. For NAD-IDH assay, the leaves were incubated in reaction solution (100 mM HEPES, pH 7.5, 5 mM $MgCl_2$, 2 mM NAD^+, 10 mM D,L-isocitrate, 0.8 mM NBT, and 0.4 mM PMS) for 3 h at 30 °C. For ABA-treated leaves, a 4-h incubation at 30 °C was performed. For NADP-IDH assay, the leaves were incubated in reaction solution (100 mM HEPES, pH 7.5, 5 mM $MgCl_2$, 1 mM $NADP^+$, 10 mM D,L-isocitrate, 0.8 mM NBT, and 0.4 mM PMS) for 3 h at 30 °C. For NADP-ME assay, the leaves were incubated in reaction solution (50 mM HEPES-KOH, pH 7.65, 1 mM $NADP^+$, 5 mM malate, 10 mM $MgSO_4$, 0.4 mM PMS, and 0.8 mM NBT) for 1 h at 30 °C. For ABA treated leaves, a 90-min incubation at 30 °C was performed.

Stomatal Aperture Measurement

Epidermal peels or intact leaves from at least four independent 3- to 4-week-old plants of various genotypes were used for stomatal closure analysis. Epidermal peels or intact leaves were floated on stomatal opening buffer (10 mM MES, pH 6.15, and 30 mM KCl) under light for 2.5 h to fully open the stomata. They were then treated with flg22 (3 μM), *Pseudomonas syringae* pv *tomato DC3000* (OD = 0.1), DEX (5 μM), COR (1 μg/mL), and ABA (10 μM) for the indicated period of time. For *MPK6SR* and *MPK3SR*, 1-(1,1-dimethylethyl)-3-(1-naphthalenyl)-1H-pyrazolo[3,4-d]pyrimidin-4-amine (NA-PP1) (2 μM final concentration) or equal volume of DMSO (solvent for NA-PP1 stock) was added at the beginning of illumination. For testing the effect of mannitol, malate, or citrate on *Pst*-induced stomatal closure, plants were dark adapted for 1 h to fully close the stomata and then were floated on MES buffer (10 mM MES, pH 6.15, and 30 mM KCl) containing mannitol (60 mM), malate (20 mM), or citrate (20 mM). Stomatal aperture was measured using ImageJ software.

Starch Staining

Leaves were floated on MES buffer (10 mM MES, pH 6.15, and 30 mM KCl) under light for 2.5 h to fully open the stomata and then were treated with either ethanol (solvent control) or DEX (5 μM) for 5 h. The treated leaves were fixed in 80% ethanol and 5% formic acid solution for 10 min at 80 °C. After being wash twice with 80% ethanol for 5 min at 80 °C each, the leaves were stained with Lugol's IKI solution (5.7 mM iodine and 43.4 mM potassium iodide) for 10 min at room temperature (Fritzius et al., 2001). Cell images were taken using an Olympus microscope fitted with a digital camera.

In Silico and Quantitative RT-PCR Analysis

Genes involved in malate metabolism and TCA cycle were retrieved from the BioCyc database (Caspi et al., 2016), and their expression levels were extracted from a previous microarray profiling analysis (Bates et al., 2012). Real-time quantitative PCR (qPCR) was performed as previously described (Mao et al., 2011). Total RNA was extracted using TRIzol reagent (Invitrogen). After DNase treatment, 1 μg of total RNA was used for reverse transcription. Real-time qPCR analysis was performed using an ABI 7500 real-time PCR machine (Life Technologies). *EF-1α* was used as an internal control. The primer pairs used for qPCR are listed in Supplemental Table 2.

Protein Extraction and Immunoblot Analysis

Protein was extracted as previously described (Liu and Zhang, 2004). Anti-Flag (Sigma-Aldrich) and anti-pTEpY (Cell Signaling Technology) antibodies were used to detect $NtMEK2^{DD}$ protein expression and MPK3/MPK6 activation, respectively.

Spectrophotometric Assay of Malate Levels

After treatment, ~0.1 g of leaf tissue was boiled in 1 mL double-distilled water for 10 min to release malate. Quantification of malate was performed as described (Peleg et al., 1990) with modifications. Two microliters of extract was used in a 100-μL reaction containing 0.6 M glycylglycine, pH 10, 0.1 M L-glutamate, 0.5 mM 3-(4,5-dimethylthiazol-2-yl)-2,5-diphenyltetrazolium bromide, 4 mM NAD^+, 0.04 mM PMS, 1 μg glutamate oxaloacetate transaminase, and 2.5 μg malate dehydrogenase for 15 min at 37 °C. The reaction was stopped by the addition of stop solution (20% SDS and 50% dimethyformamide), and the absorbance at 570 nm was measured.

Statistical Tests

For experiments with multiple time points, at least two independent repetitions were performed. For single time-point experiments, at least three independent repetitions were performed. Data from one of the independent repetitions with similar results are shown in the figures. One-way ANOVA Tukey's test was used for statistical analysis. One and two asterisks above the columns were used to indicate differences that are statistically significant ($P < 0.05$) and very significant ($P < 0.01$), respectively.

Accession Numbers

Sequence data from this article can be found in the Arabidopsis Genome Initiative or GenBank/EMBL databases under the following accession numbers: *MPK3* (At3g45640), *MPK6* (At2g43790), *MKK4* (At1g51660), *MKK5* (At3g21220), *ABA2* (At1g52340), *ABI1* (At4g26080), *OST1* (At4g33950), *SLAC1* (At1g12480), *RbohD* (At5g47910), *NADP-ME2* (At5g11670), *NADP-ME3* (At5g25880), *NADP-ME4* (At1g79750), *NAD-ME1* (At2g13560), *NAD-ME2* (At4g00570), *NAD-IDH1* (At4g35260), *NAD-IDH2* (At2g17130), *NAD-IDH5* (At5g03290), *ACS2* (At1g01480), and *EF1α* (At5g60390).

Supplemental Data

Supplemental Figure 1. Stomatal and apoplastic immunity in *mpk3* and *mpk6* single mutants.

Supplemental Figure 2. Stomatal immunity in independent *MPK3SR* and *MPK6SR* lines.

Supplemental Figure 3. Apoplastic immunity in independent *MPK3SR* and *MPK6SR* lines.

Supplemental Figure 4. Flg22- or *Pst*-induced stomatal closure was abolished in leaves of the conditional *mpk3 mpk6* double mutants.

Supplemental Figure 5. Establishing the pathogen entry assay.

Supplemental Figure 6. Stomata patterning in Col-0 and *mkk4 mkk5* double mutant.

Supplemental Figure 7. Apoplastic and stomatal immunity in *MKK4* and *MKK5* single mutants and their overexpressing lines.

Supplemental Figure 8. Loss of function of MPK3/MPK6 or their upstream MKK4/MKK5 leads to hypersensitivity to ABA-induced stomatal closure.

Supplemental Figure 9. Normal starch accumulation in guard cells of *DD* plants after DEX treatment.

Supplemental Figure 10. Activation of MPK3/MPK6 in *DD* plants or Col-0 plants after pathogen/PAMP treatment decreases total malate contents in leaves.

Supplemental Figure 11. Validation of the in situ enzyme activity assay.

Supplemental Figure 12. Quantitative RT-PCR analysis the expression of malate metabolism related genes in response to flg22 or *Pst*.

Supplemental Figure 13. *MPK3* and *MPK6* are required for *Pst*-induced activation of NADP-ME.

Supplemental Figure 14. NADP-ME and NAD-IDH activities were not affected by ABA treatment.

Supplemental Figure 15. Flg22-induced stomatal closure was not affected in *nadp-me2* mutant.

Supplemental Table 1. Expression of TCA cycle-related genes in guard cells is comparable with that in intact leaves.

Supplemental Table 2. Primers used for reverse transcription quantitative PCR analysis.

Supplemental Table 3. ANOVA tables for statistical analysis.

ACKNOWLEDGMENTS

We thank Zhizhong Gong (China Agricultural University), Dingzhong Tang (Chinese Academy of Sciences), and the Arabidopsis Biological Resource Center for mutant seeds. This work was supported by grants from the Natural Science Foundation of China (31670268 and 31272029), the 111 Project (Grant B14027), and the National Science Foundation (IOS-0743957 and MCB-0950519) to J.X. and S.Z.

AUTHOR CONTRIBUTIONS

J.S., M.Z., T.S., and L.Z. performed experiments and data analysis with substantial input from W.L., J.X., and S.Z. J.S. and S.Z. designed the experiments. J.S., J.X., and S.Z. wrote the manuscript.

Received July 21, 2016; revised February 13, 2017; accepted March 1, 2017; published March 2, 2017.

REFERENCES

Acharya, B.R., Jeon, B.W., Zhang, W., and Assmann, S.M. (2013). Open Stomata 1 (OST1) is limiting in abscisic acid responses of *Arabidopsis* guard cells. New Phytol. **200:** 1049–1063.

Anderson, J.C., Wan, Y., Kim, Y.M., Pasa-Tolic, L., Metz, T.O., and Peck, S.C. (2014). Decreased abundance of type III secretion system-inducing signals in *Arabidopsis mkp1* enhances resistance against *Pseudomonas syringae.* Proc. Natl. Acad. Sci. USA **111:** 6846–6851.

Araújo, W.L., Fernie, A.R., and Nunes-Nesi, A. (2011a). Control of stomatal aperture: a renaissance of the old guard. Plant Signal. Behav. **6:** 1305–1311.

Araújo, W.L., et al. (2011b). Antisense inhibition of the iron-sulphur subunit of succinate dehydrogenase enhances photosynthesis and growth in tomato via an organic acid-mediated effect on stomatal aperture. Plant Cell **23:** 600–627.

Arnaud, D., and Hwang, I. (2015). A sophisticated network of signaling pathways regulates stomatal defenses to bacterial pathogens. Mol. Plant **8:** 566–581.

Asai, T., Tena, G., Plotnikova, J., Willmann, M.R., Chiu, W.L., Gomez-Gomez, L., Boller, T., Ausubel, F.M., and Sheen, J. (2002). MAP kinase signalling cascade in *Arabidopsis* innate immunity. Nature **415:** 977–983.

Ausubel, F.M. (2005). Are innate immune signaling pathways in plants and animals conserved? Nat. Immunol. **6:** 973–979.

Azoulay-Shemer, T., Bagheri, A., Wang, C., Palomares, A., Stephan, A.B., Kunz, H.H., and Schroeder, J.I. (2016). Starch biosynthesis in guard cells but not in mesophyll cells is involved in CO_2-induced stomatal closing. Plant Physiol. **171:** 788–798.

Banks, A.S., McAllister, F.E., Camporez, J.P.G., Zushin, P.-J.H., Jurczak, M.J., Laznik-Bogoslavski, D., Shulman, G.I., Gygi, S.P., and Spiegelman, B.M. (2015). An ERK/Cdk5 axis controls the diabetogenic actions of PPARγ. Nature **517:** 391–395.

Bates, G.W., Rosenthal, D.M., Sun, J., Chattopadhyay, M., Peffer, E., Yang, J., Ort, D.R., and Jones, A.M. (2012). A comparative study of the *Arabidopsis thaliana* guard-cell transcriptome and its modulation by sucrose. PLoS One **7:** e49641.

Baud, S., and Graham, I.A. (2006). A spatiotemporal analysis of enzymatic activities associated with carbon metabolism in wild-type and mutant embryos of *Arabidopsis* using *in situ* histochemistry. Plant J. **46:** 155–169.

Beckers, G.J., Jaskiewicz, M., Liu, Y., Underwood, W.R., He, S.Y., Zhang, S., and Conrath, U. (2009). Mitogen-activated protein kinases 3 and 6 are required for full priming of stress responses in *Arabidopsis thaliana.* Plant Cell **21:** 944–953.

Berriri, S., Garcia, A.V., Frei dit Frey, N., Rozhon, W., Pateyron, S., Leonhardt, N., Montillet, J.L., Leung, J., Hirt, H., and Colcombet, J. (2012). Constitutively active mitogen-activated protein kinase versions reveal functions of *Arabidopsis* MPK4 in pathogen defense signaling. Plant Cell **24:** 4281–4293.

Blatt, M.R. (2016). Plant physiology: Redefining the enigma of metabolism in stomatal movement. Curr. Biol. **26:** R107–R109.

Böhm, H., Albert, I., Fan, L., Reinhard, A., and Nürnberger, T. (2014). Immune receptor complexes at the plant cell surface. Curr. Opin. Plant Biol. **20:** 47–54.

Boller, T., and Felix, G. (2009). A renaissance of elicitors: perception of microbe-associated molecular patterns and danger signals by pattern-recognition receptors. Annu. Rev. Plant Biol. **60:** 379–406.

Brandt, B., et al. (2015). Calcium specificity signaling mechanisms in abscisic acid signal transduction in *Arabidopsis* guard cells. eLife **4:** e03599.

Brooks, D.M., Hernández-Guzmán, G., Kloek, A.P., Alarcón-Chaidez, F., Sreedharan, A., Rangaswamy, V., Peñaloza-Vázquez, A., Bender, C.L., and Kunkel, B.N. (2004). Identification and characterization of a well-defined series of coronatine biosynthetic mutants of *Pseudomonas syringae* pv. *tomato DC3000.* Mol. Plant Microbe Interact. **17:** 162–174.

Caspi, R., et al. (2016). The MetaCyc database of metabolic pathways and enzymes and the BioCyc collection of pathway/genome databases. Nucleic Acids Res. **44:** D471–D480.

Chater, C.C., Oliver, J., Casson, S., and Gray, J.E. (2014). Putting the brakes on: abscisic acid as a central environmental regulator of stomatal development. New Phytol. **202:** 376–391.

Chisholm, S.T., Coaker, G., Day, B., and Staskawicz, B.J. (2006). Host-microbe interactions: shaping the evolution of the plant immune response. Cell **124:** 803–814.

Choi, J.H., Banks, A.S., Estall, J.L., Kajimura, S., Boström, P., Laznik, D., Ruas, J.L., Chalmers, M.J., Kamenecka, T.M., Blüher, M., Griffin, P.R., and Spiegelman, B.M. (2010). Anti-diabetic drugs inhibit obesity-linked phosphorylation of PPARgamma by Cdk5. Nature **466:** 451–456.

Cuppels, D.A., and Ainsworth, T. (1995). Molecular and physiological characterization of *Pseudomonas syringae* pv. *tomato* and *Pseudomonas syringae* pv. *maculicola* strains that produce the phytotoxin coronatine. Appl. Environ. Microbiol. **61:** 3530–3536.

Daloso, D.M., Antunes, W.C., Pinheiro, D.P., Waquim, J.P., Araújo, W.L., Loureiro, M.E., Fernie, A.R., and Williams, T.C. (2015). Tobacco guard cells fix CO_2 by both Rubisco and PEPcase while sucrose acts as a substrate during light-induced stomatal opening. Plant Cell Environ. **38:** 2353–2371.

Doehlemann, G., and Hemetsberger, C. (2013). Apoplastic immunity and its suppression by filamentous plant pathogens. New Phytol. **198:** 1001–1016.

Du, M., et al. (2014). Closely related NAC transcription factors of tomato differentially regulate stomatal closure and reopening during pathogen attack. Plant Cell **26:** 3167–3184.

Fan, J., Crooks, C., and Lamb, C. (2008). High-throughput quantitative luminescence assay of the growth in planta of *Pseudomonas syringae* chromosomally tagged with *Photorhabdus luminescens* luxCDABE. Plant J. **53:** 393–399.

Fritzius, T., Aeschbacher, R., Wiemken, A., and Wingler, A. (2001). Induction of ApL3 expression by trehalose complements the starch-deficient *Arabidopsis* mutant *adg2-1* lacking ApL1, the large subunit of ADP-glucose pyrophosphorylase. Plant Physiol. **126:** 883–889.

Geiger, D., Scherzer, S., Mumm, P., Stange, A., Marten, I., Bauer, H., Ache, P., Matschi, S., Liese, A., Al-Rasheid, K.A., Romeis, T., and Hedrich, R. (2009). Activity of guard cell anion channel SLAC1 is controlled by drought-stress signaling kinase-phosphatase pair. Proc. Natl. Acad. Sci. USA **106:** 21425–21430.

Gilliham, M., and Tyerman, S.D. (2016). Linking metabolism to membrane signaling: The GABA-malate connection. Trends Plant Sci. **21:** 295–301.

González-Guzmán, M., Apostolova, N., Bellés, J.M., Barrero, J.M., Piqueras, P., Ponce, M.R., Micol, J.L., Serrano, R., and Rodríguez, P.L. (2002). The short-chain alcohol dehydrogenase ABA2 catalyzes the conversion of xanthoxin to abscisic aldehyde. Plant Cell **14:** 1833–1846.

Grimmer, M.K., John Foulkes, M., and Paveley, N.D. (2012). Foliar pathogenesis and plant water relations: a review. J. Exp. Bot. **63:** 4321–4331.

Guan, R., Su, J., Meng, X., Li, S., Liu, Y., Xu, J., and Zhang, S. (2015). Multilayered regulation of ethylene induction plays a positive role in *Arabidopsis* resistance against *Pseudomonas syringae.* Plant Physiol. **169:** 299–312.

Gudesblat, G.E., Torres, P.S., and Vojnov, A.A. (2009). *Xanthomonas campestris* overcomes *Arabidopsis* stomatal innate immunity through a DSF cell-to-cell signal-regulated virulence factor. Plant Physiol. **149:** 1017–1027.

Guimarães, R.L., and Stotz, H.U. (2004). Oxalate production by *Sclerotinia sclerotiorum* deregulates guard cells during infection. Plant Physiol. **136:** 3703–3711.

Guzel Deger, A., Scherzer, S., Nuhkat, M., Kedzierska, J., Kollist, H., Brosché, M., Unyayar, S., Boudsocq, M., Hedrich, R., and Roelfsema, M.R. (2015). Guard cell SLAC1-type anion channels mediate flagellin-induced stomatal closure. New Phytol. **208:** 162–173.

Hetherington, A.M., and Woodward, F.I. (2003). The role of stomata in sensing and driving environmental change. Nature **424:** 901–908.

Horrer, D., Flütsch, S., Pazmino, D., Matthews, J.S., Thalmann, M., Nigro, A., Leonhardt, N., Lawson, T., and Santelia, D. (2016). Blue light induces a distinct starch degradation pathway in guard cells for stomatal opening. Curr. Biol. **26:** 362–370.

Hosy, E., et al. (2003). The *Arabidopsis* outward K^+ channel GORK is involved in regulation of stomatal movements and plant transpiration. Proc. Natl. Acad. Sci. USA **100:** 5549–5554.

Hua, D., Wang, C., He, J., Liao, H., Duan, Y., Zhu, Z., Guo, Y., Chen, Z., and Gong, Z. (2012). A plasma membrane receptor kinase, GHR1, mediates abscisic acid- and hydrogen peroxide-regulated stomatal movement in *Arabidopsis.* Plant Cell **24:** 2546–2561.

Hurley, B., Lee, D., Mott, A., Wilton, M., Liu, J., Liu, Y.C., Angers, S., Coaker, G., Guttman, D.S., and Desveaux, D. (2014). The *Pseudomonas syringae* type III effector HopF2 suppresses *Arabidopsis* stomatal immunity. PLoS One **9:** e114921.

Jammes, F., Yang, X., Xiao, S., and Kwak, J.M. (2011). Two *Arabidopsis* guard cell-preferential MAPK genes, *MPK9* and *MPK12*, function in biotic stress response. Plant Signal. Behav. **6:** 1875–1877.

Jammes, F., et al. (2009). MAP kinases MPK9 and MPK12 are preferentially expressed in guard cells and positively regulate ROS-mediated ABA signaling. Proc. Natl. Acad. Sci. USA **106:** 20520–20525.

Jinno, N.F.M. (1981). Effects of calcium-complexing agents, sodium oxalate and soduim citrate on stomatal opening and closing of *Commelina communis L*. Nagasaki University **32:** 83–86.

Johansson, F., Sommarin, M., and Larsson, C. (1993). Fusicoccin activates the plasma membrane H^+-ATPase by a mechanism involving the C-terminal inhibitory domain. Plant Cell **5:** 321–327.

Jones, J.D., and Dangl, J.L. (2006). The plant immune system. Nature **444:** 323–329.

Kadota, Y., Sklenar, J., Derbyshire, P., Stransfeld, L., Asai, S., Ntoukakis, V., Jones, J.D., Shirasu, K., Menke, F., Jones, A., and Zipfel, C. (2014). Direct regulation of the NADPH oxidase RBOHD by the PRR-associated kinase BIK1 during plant immunity. Mol. Cell **54:** 43–55.

Kelly, G., Moshelion, M., David-Schwartz, R., Halperin, O., Wallach, R., Attia, Z., Belausov, E., and Granot, D. (2013). Hexokinase mediates stomatal closure. Plant J. **75:** 977–988.

Kim, T.H., Böhmer, M., Hu, H., Nishimura, N., and Schroeder, J.I. (2010). Guard cell signal transduction network: advances in understanding abscisic acid, CO_2, and Ca^{2+} signaling. Annu. Rev. Plant Biol. **61:** 561–591.

Kim, T.H., et al. (2011). Chemical genetics reveals negative regulation of abscisic acid signaling by a plant immune response pathway. Curr. Biol. **21:** 990–997.

Lawson, T. (2009). Guard cell photosynthesis and stomatal function. New Phytol. **181:** 13–34.

Lee, J.S., Wang, S., Sritubtim, S., Chen, J.G., and Ellis, B.E. (2009). *Arabidopsis* mitogen-activated protein kinase MPK12 interacts with

the MAPK phosphatase IBR5 and regulates auxin signaling. Plant J. **57:** 975–985.

Lee, M., Choi, Y., Burla, B., Kim, Y.Y., Jeon, B., Maeshima, M., Yoo, J.Y., Martinoia, E., and Lee, Y. (2008). The ABC transporter AtABCB14 is a malate importer and modulates stomatal response to CO_2. Nat. Cell Biol. **10:** 1217–1223.

Lemaitre, T., Urbanczyk-Wochniak, E., Flesch, V., Bismuth, E., Fernie, A.R., and Hodges, M. (2007). NAD-dependent isocitrate dehydrogenase mutants of *Arabidopsis* suggest the enzyme is not limiting for nitrogen assimilation. Plant Physiol. **144:** 1546–1558.

Li, L., Li, M., Yu, L., Zhou, Z., Liang, X., Liu, Z., Cai, G., Gao, L., Zhang, X., Wang, Y., Chen, S., and Zhou, J.M. (2014). The FLS2-associated kinase BIK1 directly phosphorylates the NADPH oxidase RbohD to control plant immunity. Cell Host Microbe **15:** 329–338.

Li, S., Mhamdi, A., Clement, C., Jolivet, Y., and Noctor, G. (2013). Analysis of knockout mutants suggests that *Arabidopsis* NADP-MALIC ENZYME2 does not play an essential role in responses to oxidative stress of intracellular or extracellular origin. J. Exp. Bot. **64:** 3605–3614.

Lim, C.W., Luan, S., and Lee, S.C. (2014). A prominent role for RCAR3-mediated ABA signaling in response to *Pseudomonas syringae* pv. *tomato DC3000* infection in *Arabidopsis.* Plant Cell Physiol. **55:** 1691–1703.

Liu, Y., and Zhang, S. (2004). Phosphorylation of 1-aminocyclopropane-1-carboxylic acid synthase by MPK6, a stress-responsive mitogen-activated protein kinase, induces ethylene biosynthesis in *Arabidopsis.* Plant Cell **16:** 3386–3399.

Lozano-Durán, R., Bourdais, G., He, S.Y., and Robatzek, S. (2014). The bacterial effector HopM1 suppresses PAMP-triggered oxidative burst and stomatal immunity. New Phytol. **202:** 259–269.

Mao, G., Meng, X., Liu, Y., Zheng, Z., Chen, Z., and Zhang, S. (2011). Phosphorylation of a WRKY transcription factor by two pathogen-responsive MAPKs drives phytoalexin biosynthesis in *Arabidopsis.* Plant Cell **23:** 1639–1653.

McLachlan, D.H., Kopischke, M., and Robatzek, S. (2014). Gate control: guard cell regulation by microbial stress. New Phytol. **203:** 1049–1063.

McLachlan, D.H., Lan, J., Geilfus, C.M., Dodd, A.N., Larson, T., Baker, A., Hõrak, H., Kollist, H., He, Z., Graham, I., Mickelbart, M.V., and Hetherington, A.M. (2016). The breakdown of stored triacylglycerols is required during light-induced stomatal opening. Curr. Biol. **26:** 707–712.

Melotto, M., Underwood, W., and He, S.Y. (2008). Role of stomata in plant innate immunity and foliar bacterial diseases. Annu. Rev. Phytopathol. **46:** 101–122.

Melotto, M., Underwood, W., Koczan, J., Nomura, K., and He, S.Y. (2006). Plant stomata function in innate immunity against bacterial invasion. Cell **126:** 969–980.

Meng, X., and Zhang, S. (2013). MAPK cascades in plant disease resistance signaling. Annu. Rev. Phytopathol. **51:** 245–266.

Menke, F.L., van Pelt, J.A., Pieterse, C.M., and Klessig, D.F. (2004). Silencing of the mitogen-activated protein kinase MPK6 compromises disease resistance in *Arabidopsis.* Plant Cell **16:** 897–907.

Meyer, S., Mumm, P., Imes, D., Endler, A., Weder, B., Al-Rasheid, K.A., Geiger, D., Marten, I., Martinoia, E., and Hedrich, R. (2010). AtALMT12 represents an R-type anion channel required for stomatal movement in *Arabidopsis* guard cells. Plant J. **63:** 1054–1062.

Mhamdi, A., Mauve, C., Gouia, H., Saindrenan, P., Hodges, M., and Noctor, G. (2010). Cytosolic NADP-dependent isocitrate dehydrogenase contributes to redox homeostasis and the regulation of pathogen responses in *Arabidopsis* leaves. Plant Cell Environ. **33:** 1112–1123.

Monaghan, J., and Zipfel, C. (2012). Plant pattern recognition receptor complexes at the plasma membrane. Curr. Opin. Plant Biol. **15:** 349–357.

Montillet, J.L., et al. (2013). An abscisic acid-independent oxylipin pathway controls stomatal closure and immune defense in *Arabidopsis.* PLoS Biol. **11:** e1001513.

Mustilli, A.C., Merlot, S., Vavasseur, A., Fenzi, F., and Giraudat, J. (2002). *Arabidopsis* OST1 protein kinase mediates the regulation of stomatal aperture by abscisic acid and acts upstream of reactive oxygen species production. Plant Cell **14:** 3089–3099.

Nagy, S.K., Darula, Z., Kállai, B.M., Bögre, L., Bánhegyi, G., Medzihradszky, K.F., Horváth, G.V., and Mészáros, T. (2015). Activation of AtMPK9 through autophosphorylation that makes it independent of the canonical MAPK cascades. Biochem. J. **467:** 167–175.

Negi, J., Matsuda, O., Nagasawa, T., Oba, Y., Takahashi, H., Kawai-Yamada, M., Uchimiya, H., Hashimoto, M., and Iba, K. (2008). CO_2 regulator SLAC1 and its homologues are essential for anion homeostasis in plant cells. Nature **452:** 483–486.

Peleg, Y., Rokem, J.S., and Goldberg, I. (1990). A simple plate-assay for the screening of L-malic acid producing microorganisms. FEMS Microbiol. Lett. **55:** 233–236.

Ramesh, S.A., et al. (2015). GABA signalling modulates plant growth by directly regulating the activity of plant-specific anion transporters. Nat. Commun. **6:** 7879. Erratum. Nat. Commun. 6: 8293.

Ren, D., Yang, H., and Zhang, S. (2002). Cell death mediated by MAPK is associated with hydrogen peroxide production in *Arabidopsis.* J. Biol. Chem. **277:** 559–565.

Ren, D., Liu, Y., Yang, K.Y., Han, L., Mao, G., Glazebrook, J., and Zhang, S. (2008). A fungal-responsive MAPK cascade regulates phytoalexin biosynthesis in *Arabidopsis.* Proc. Natl. Acad. Sci. USA **105:** 5638–5643.

Ruszala, E.M., Beerling, D.J., Franks, P.J., Chater, C., Casson, S.A., Gray, J.E., and Hetherington, A.M. (2011). Land plants acquired active stomatal control early in their evolutionary history. Curr. Biol. **21:** 1030–1035.

Sasaki, T., Mori, I.C., Furuichi, T., Munemasa, S., Toyooka, K., Matsuoka, K., Murata, Y., and Yamamoto, Y. (2010). Closing plant stomata requires a homolog of an aluminum-activated malate transporter. Plant Cell Physiol. **51:** 354–365.

Sirichandra, C., Gu, D., Hu, H.C., Davanture, M., Lee, S., Djaoui, M., Valot, B., Zivy, M., Leung, J., Merlot, S., and Kwak, J.M. (2009). Phosphorylation of the *Arabidopsis* AtrbohF NADPH oxidase by OST1 protein kinase. FEBS Lett. **583:** 2982–2986.

Tanaka, Y., Sano, T., Tamaoki, M., Nakajima, N., Kondo, N., and Hasezawa, S. (2006). Cytokinin and auxin inhibit abscisic acid-induced stomatal closure by enhancing ethylene production in *Arabidopsis.* J. Exp. Bot. **57:** 2259–2266.

Torres, M.A., Dangl, J.L., and Jones, J.D. (2002). *Arabidopsis* gp91phox homologues AtrbohD and AtrbohF are required for accumulation of reactive oxygen intermediates in the plant defense response. Proc. Natl. Acad. Sci. USA **99:** 517–522.

Tronconi, M.A., Fahnenstich, H., Gerrard Weehler, M.C., Andreo, C.S., Flügge, U.I., Drincovich, M.F., and Maurino, V.G. (2008). *Arabidopsis* NAD-malic enzyme functions as a homodimer and heterodimer and has a major impact on nocturnal metabolism. Plant Physiol. **146:** 1540–1552.

Tsuda, K., Mine, A., Bethke, G., Igarashi, D., Botanga, C.J., Tsuda, Y., Glazebrook, J., Sato, M., and Katagiri, F. (2013). Dual regulation of gene expression mediated by extended MAPK activation and salicylic acid contributes to robust innate immunity in *Arabidopsis thaliana.* PLoS Genet. **9:** e1004015.

Vahisalu, T., Kollist, H., Wang, Y.F., Nishimura, N., Chan, W.Y., Valerio, G., Lamminmäki, A., Brosché, M., Moldau, H., Desikan, R., Schroeder, J.I., and Kangasjärvi, J. (2008). SLAC1 is required for plant guard cell S-type anion channel function in stomatal signalling. Nature **452:** 487–491.

Wang, H., Ngwenyama, N., Liu, Y., Walker, J.C., and Zhang, S. (2007). Stomatal development and patterning are regulated by environmentally responsive mitogen-activated protein kinases in *Arabidopsis*. Plant Cell **19:** 63–73.

Wheeler, M.C., Tronconi, M.A., Drincovich, M.F., Andreo, C.S., Flügge, U.I., and Maurino, V.G. (2005). A comprehensive analysis of the NADP-malic enzyme gene family of *Arabidopsis*. Plant Physiol. **139:** 39–51.

Xu, J., and Zhang, S. (2015). Mitogen-activated protein kinase cascades in signaling plant growth and development. Trends Plant Sci. **20:** 56–64.

Xu, J., Xie, J., Yan, C., Zou, X., Ren, D., and Zhang, S. (2014). A chemical genetic approach demonstrates that MPK3/MPK6 activation and NADPH oxidase-mediated oxidative burst are two independent signaling events in plant immunity. Plant J. **77:** 222–234.

Xu, J., Meng, J., Meng, X., Zhao, Y., Liu, J., Sun, T., Liu, Y., Wang, Q., and Zhang, S. (2016). Pathogen-responsive MPK3 and MPK6 reprogram the biosynthesis of indole glucosinolates and their derivatives in *Arabidopsis* immunity. Plant Cell **28:** 1144–1162.

Zeng, W., and He, S.Y. (2010). A prominent role of the flagellin receptor FLAGELLIN-SENSING2 in mediating stomatal response to *Pseudomonas syringae* pv *tomato DC3000* in *Arabidopsis*. Plant Physiol. **153:** 1188–1198.

Zhang, S., and Klessig, D.F. (2001). MAPK cascades in plant defense signaling. Trends Plant Sci. **6:** 520–527.

Zhang, W., Nilson, S.E., and Assmann, S.M. (2008). Isolation and whole-cell patch clamping of *Arabidopsis* guard cell protoplasts. CSH Protoc. **2008:** pdb.prot5014.

Zhao, C., Nie, H., Shen, Q., Zhang, S., Lukowitz, W., and Tang, D. (2014). EDR1 physically interacts with MKK4/MKK5 and negatively regulates a MAP kinase cascade to modulate plant innate immunity. PLoS Genet. **10:** e1004389.

Zheng, X.Y., Zhou, M., Yoo, H., Pruneda-Paz, J.L., Spivey, N.W., Kay, S.A., and Dong, X. (2015). Spatial and temporal regulation of biosynthesis of the plant immune signal salicylic acid. Proc. Natl. Acad. Sci. USA **112:** 9166–9173.

Zheng, X.Y., Spivey, N.W., Zeng, W., Liu, P.P., Fu, Z.Q., Klessig, D.F., He, S.Y., and Dong, X. (2012). Coronatine promotes *Pseudomonas syringae* virulence in plants by activating a signaling cascade that inhibits salicylic acid accumulation. Cell Host Microbe **11:** 587–596.